OCS Study
MMS 93-0044

University Research Initiative

Satellite Assessment of Mississippi River Discharge Plume Variability

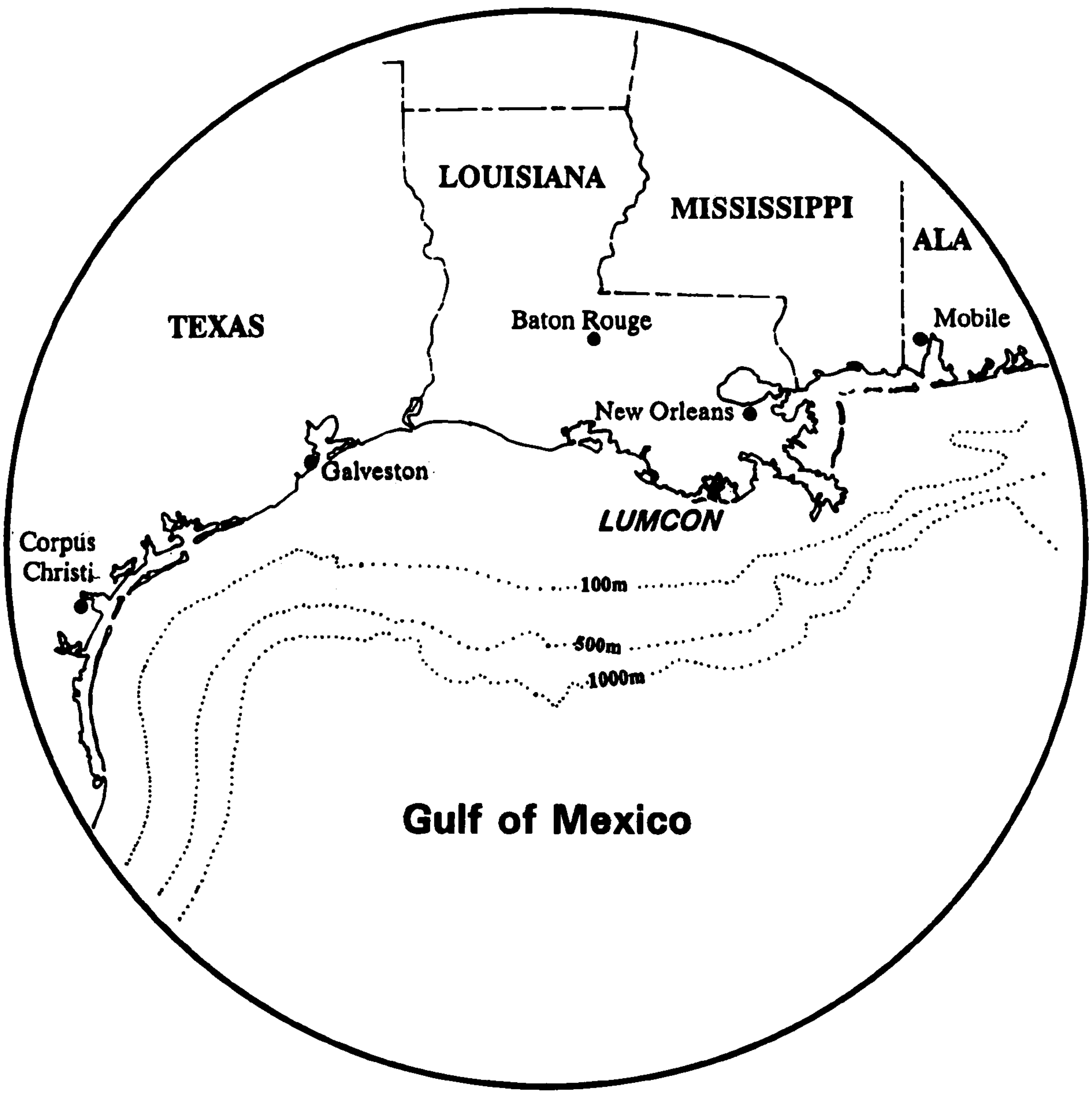

MMS
U.S. Department of the Interior
Minerals Management Service
Gulf of Mexico OCS Region

LUMCON
Cooperative Agreement
University Research Initiative
Louisiana Universities Marine Consortium

OCS Study
MMS 93-0044

University Research Initiative

Satellite Assessment of Mississippi River Discharge Plume Variability

Authors

Nan D. Walker
Lawrence J. Rouse, Jr.
Coastal Studies Institute
Louisiana State University
Baton Rouge, Louisiana

October 1993

Prepared under MMS Contract
14-35-0001-30470
by
Louisiana Universities Marine Consortium
150 Riverside Mall, Room 107
Baton Rouge, Louisiana 70801

Published by

U.S. Department of the Interior
Minerals Management Service
Gulf of Mexico OCS Region

Cooperative Agreement
University Research Initiative
Louisiana Universities Marine Consortium

DISCLAIMER

This report was prepared under contract between the Minerals Management Service (MMS) and the Coastal Studies Institutes, Louisiana State University. This report has been technically reviewed by the MMS and approved for publication. Approval does not signify that the contents necessarily reflect the views and policies of the Service, nor does mention of trade names or commercial products constitute endorsement or recommendation for use. It is, however, exempt from review and compliance with MMS editorial standards.

REPORT AVAILABILITY

Extra copies of the report may be obtained from the Public Information Unit (Mail Stop 5034) at the following address:

U.S. Department of the Interior
Minerals Management Service
Gulf of Mexico OCS Regional Office
Public Information Unit (MS 5034)
1201 Elmwood Park Boulevard
New Orleans, Louisiana 70123-2394
Telephone Number: (504) 736-2519

CITATION

Walker, N.D. and L.J. Rouse, Jr. 1993. Satellite assessment of Mississippi River discharge plume variability. OCS Study MMS 93-0044. U.S. Dept. of the Interior, Minerals Management Service, Gulf of Mexico OCS Regional Office, New Orleans, La. 50 pp.

ABSTRACT

The Mississippi River is the major contributor of sediments, pollutants, and nutrients to the northern Gulf of Mexico continental shelf and slope. This study utilized four years of NOAA Advanced Very High Resolution Radiometer (AVHRR) satellite data to quantify which areas of the continental shelf and slope of the Gulf of Mexico are subjected to Mississippi River discharges. The eighty-three images analyzed revealed that the sediment plume varied greatly in size, from 450 km^2 to 7700 km^2. River discharge was found to exert some control over plume size; however, wind speed and direction were also important controlling factors in determining plume morphology and surface sediment distribution over the continental shelf and slope. Results of a compositing analysis revealed that under medium discharge conditions, the "mean" composite plume covered 2200 km^2 of the continental shelf. Under high discharge conditions, the area of the "mean" composite plume doubled. The spatial extent of the "maximum" composite plume under high discharge conditions covered an extensive area of the continental shelf and slope (13,207 km^2), extending from 88° 20' W to 90° 50' W, and offshore to the 1000 m isobath. Although the freshwater and sediments of the Mississippi River plume were generally confined to the continental shelf, substantial cross-shelf and shelf-slope exchanges of plume water occurred during strong wind events. Off-shelf movement of river water was initiated by strong winds from the west through northeast. Subsequently, the movement of river water over the continental slope was controlled primarily by slope currents, often associated with Loop Current eddies and filaments.

This study has revealed that the proportion of water flowing westward from the eastern side of the delta may increase from October through March, as a result of cold-front passages. Under the influence of strong northeasterly winds, river water from the eastern passes and ambient coastal waters flow southward hugging the eastern delta region. They subsequently turn westward to join the discharge emanating from South Pass and Southwest Pass. Sediment transport towards the southeast and east is often inhibited by strong convergence zones associated with the prevailing southeasterly wind regime as well as by intrusions of the Loop Current water onto the shelf. To the west of the delta, the shelf circulation is generally anticyclonic within the Louisiana Bight although a portion of the plume often flows further westward. The net result is an accumulation of river sediments, pollutants and nutrients within the bight and on the shelf west of Southwest Pass.

TABLE OF CONTENTS

LIST OF FIGURES

LIST OF TABLES

ACKNOWLEDGMENTS

Many thanks are extended to Dr. Oscar Huh, Director of the Earth Scan Lab, and Dr. Lawrence Rouse, Jr., Assistant Director, for providing the four years of data for this project and also for fruitful discussions in the course of this study. Thanks are also extended to David Wilensky, Systems Manager of the Earth Scan Lab, for making it all work and for computer software developments in support of this project. Varis Ransibrahmanakul is gratefully acknowledged for his assistance with software development and both Varis and David are thanked for assisting with the field data collection. The following undergraduate students deserve medals for their monumental efforts in screening the historic satellite data archive: Mellissa Seymour, Adele Babin, Jenny Roth, Rita Creasy, and Christa Babin. Scott Lear and Bridget Fredericks were invaluable assistants with various image processing tasks and their help is acknowledged with much gratitude. This report was produced through the PC ingenuity of Bridget Fredericks, to whom I extend a special thanks.

The Grand Isle wind data was provided by Dr. William Wiseman and was made available for analysis by Laura Carriere, both of whom are acknowledged for their assistance. Eric Meindel of the National Data Buoy Center is thanked for providing Grand Isle wind data during 1992. Eddy Weeks is thanked for assisting in the wind data processing. The U.S. Army Corps of Engineers, New Orleans District, and the U.S. Geological Survey are acknowledged for providing river discharge, sediment discharge and suspended sediment data. Last but not least, Rob Cunningham of the U.S. Army Corps of Engineers, New Orleans District, is gratefully acknowledged for his advice on field sampling from a helicopter and also for providing discharge information.

INTRODUCTION

The Mississippi River is the major source of fresh water, sediments, nutrients and pollutants for the Gulf of Mexico. Draining 41% of the continental U.S., it discharges freshwater into the northern Gulf of Mexico through the bird-foot delta region at an average rate of 14,000 $m^3 \cdot s^{-1}$ Mossa (1990) and, in addition, transports about 150 million tons of sediment to the Gulf annually (Milliman and Meade 1983). The Atchafalaya River (the major distributary of the Mississippi River) carries approximately one-half of this amount. Although the Mississippi River is the largest river in North America and 6th largest worldwide in terms of discharge (Milliman and Meade, 1983) few studies have focused on the fate of river water once it enters the Gulf of Mexico.

Satellite-acquired data can provide valuable information on the distribution of river water and sediments on the continental shelf as well as on the circulation processes affecting the fate of riverborne sediments and pollutants. This type of data yields synoptic coverage over large geographic areas, unattainable from research ships or moorings. Numerous investigators have utilized satellite data as the primary data source in studying river systems, estuaries and the interaction of river plumes with oceanic water (Rouse and Coleman 1976, Gagliardini et al. 1984, Schroeder et al. 1985, Stumpf 1988, Muller-Karger et al. 1988, Dinnel et al. 1990).

This report presents the findings of a one-year study on Mississippi River discharge plume variability. The study has been based on the analysis and interpretation of multi-year data obtained by the Advanced Very High Resolution Radiometer (AVHRR) aboard the National Oceanographic and Atmospheric Administration (NOAA) series of environmental satellites.

The primary objective of this study was to determine which areas of the continental shelf and slope in the Gulf of Mexico are most influenced by riverborne sediments, pollutants and nutrients carried by the Mississippi River through the Balize delta region. An additional objective was to gain a better understanding of the environmental forcing factors controlling the distribution of river water and sediments within the northern Gulf of Mexico. With the exception of the pioneering work of Rouse and Coleman (1976) using LANDSAT data, no studies of this type have focused on the Mississippi River plume region. Therefore, this study should provide important baseline information of use to environmental managers and researchers in wide-ranging fields of oceanography and hydrology.

BACKGROUND INFORMATION

The Mississippi River discharges into the northern Gulf of Mexico through the Balize (bird-foot) and Atchafalaya delta regions (Figure 1). Flow down the Atchafalaya River is limited to 30% of the total Mississippi River flow by the Old River Control Structure. The total annual discharge of the Mississippi/Atchafalaya River system is 507 km^3 which amounts to 10% of the volume of the entire Louisiana-Texas shelf out to the 90 meter bathymetric contour (Dinnel and Wiseman 1986, Dagg and Whitledge 1991). The freshwater influence from these rivers has been observed as far as Port Aransas, Texas, a distance of 800 km from the Mississippi River Balize delta (Smith 1980).

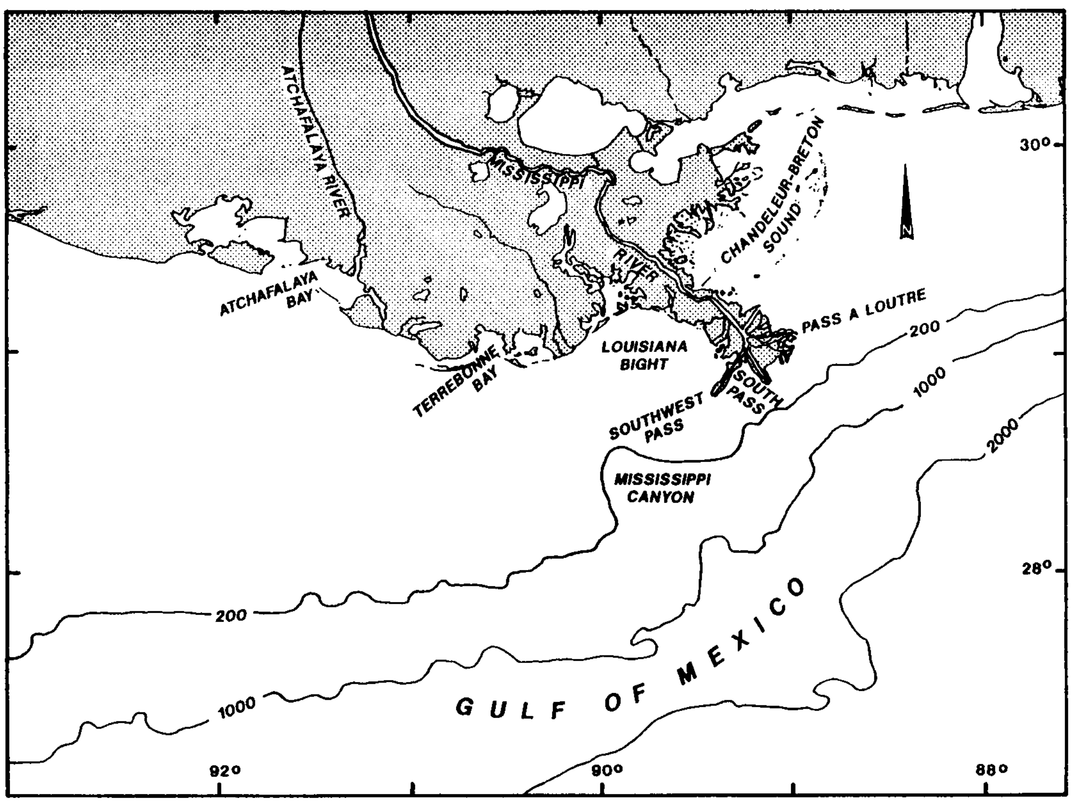

Figure 1. Map of the main study area. Contours are in meters.

The inputs of freshwater, sediment, nutrients and pollutants have a major impact on all aspects of continental shelf oceanography in the northern Gulf of Mexico. The input of nutrients ensures that the region surrounding the Mississippi River delta is highly productive in terms of phytoplankton and zooplankton production (Dagg et al. 1987, Lohrenz et al. 1990). Research results of Walsh et al. (1989) suggest that the Mississippi plume area is the most productive within the Gulf of Mexico. The entire Louisiana/Texas shelf supports a very productive fishery which amounts to 28% of the total U.S. catch (Rabalais et al. 1991) and spawning of key species, such as Gulf menhaden (Brevortia patronus), is concentrated around the Mississippi Delta (Sogard et al. 1987). There are negative consequences of the high productivity in that a large zone of hypoxia is generated during summer months over much of the Louisiana continental shelf west of the Balize delta (Rabalais et al. 1991). In addition to the nutrient input, the fine-grained river sediments in suspension carry an abundance of pollutants, which are potentially dangerous to fish and shellfish (Jay Means, Professor, Environmental Chemistry and Toxicology, Louisiana State University, personal communication). Approximately 90% of sediment within the river is transported as suspended load (Fisk et al. 1954); of which, 40% typically consists of silt, 50% of clay and 10% of very fine sand (Wright and Coleman 1974). Sediment is an important resource to Louisiana, the state which is experiencing the highest land loss rates in the United States. Results of this study will provide important information concerning the distribution of sediment on the continental shelf which should enable more effective management of Mississippi River sediments.

This study concentrates on the fate of the Mississippi River discharge through the Balize delta region, which includes approximately 70% of the entire flow. South of Venice, at Head of Passes, the Mississippi River branches into three major distributaries: Southwest Pass, South Pass, and Pass a Loutre. The percentage flow through these main distributaries has been estimated at 30%, 15%, and 30% , respectively (U.S. Army Corps of Engineers 1984). The remaining 25% is discharged through secondary channels.

At the mouths of the passes, the river experiences buoyant expansion and mixing due to wave, wind and tidal currents on the continental shelf (Wright and Coleman 1974). The freshwater "plume" produces a halocline within the upper 10 meters even when cold water overlies warm (Wiseman and Dinnel 1988). The thickness of the freshwater "lens" which overlies more saline ambient Gulf water increases with increasing river discharge and under the presence of wave-induced mixing (Wright 1970). Stratification of the water column generally increases with increasing discharge (usually in spring) and in association with weak winds of summer (Rabalais et al. 1991). Strong thermal and color fronts are often observed on the south and east sides of the Balize delta region as a result of convergence of river water with ambient Gulf water (Wright and Coleman 1974). Wright and Coleman (1971) found a band of shelf water of intermediate salinity between the river water and ambient Gulf water which they suggested originated from passes to the northeast of South Pass.

Circulation on the inner continental shelf near the Balize delta is primarily wind-driven (Murray 1972, Schroeder et al. 1987). The prevailing winds offshore of the delta are easterly; southeasterly from March through September and northeasterly from October through February

(Rhodes et al. 1985). Thus, the wind-driven surface currents are primarily westward. In addition, the nearshore pressure gradient set up by river runoff drives a westward geostrophic flow near the coast (Schroeder et al. 1987) which enhances the wind-induced westward current. From October through March, cold front passages perturb the prevailing easterly wind regime. They occur every 3 to 10 days (Fernandez-Partegas and Mooers 1975) and are characterized by a clockwise rotation in the wind field; from southeast to southwest, northwest, and northeast. Strongest winds usually blow from the northerly quadrants. Winds associated with cold-front passages have important effects on shelf circulation (Huh et al. 1978, Schroeder et al. 1987, Wiseman and Dinnel 1988). In addition, Loop Current filaments and eddies can affect circulation in the vicinity of the Balize delta (Wiseman and Dinnel 1988, Ebbesmeyer et al. 1982). Shelf currents in excess of 2 $m \cdot s^{-1}$ have been caused by the intrusion of Loop Current filaments onto the shelf and slope where they have seriously disrupted oil and gas activities in the northern Gulf of Mexico (Huh and Schaudt 1990).

The Balize delta extends nearly completely across the Mississippi/Louisiana continental shelf, essentially blocking the shelf to significant amounts of east-west flow (Wiseman and Dinnel 1988). Chew et al. (1962) suggest that a saddle point in the general Gulf circulation exists in front of the delta, with eastward flow occurring along the shelf edge east of the delta and westward flow occurring west of the delta. Schroeder et al. (1987) concur with the suggestion of Chew et al. (1962) and also report the existence of anti-clockwise circulation on the shelf east of the delta with westward flow along the inner shelf in approximately 20-30 meters of water. Also in agreement with Chew et al. (1962), Cochrane and Kelly (1986) and Wiseman et al. (1976) report westward outer shelf flow west of the delta. On the inner shelf west of the delta, in the Louisiana Bight, a clockwise circulation has been previously reported (Wiseman et al. 1976, Rouse and Coleman 1976). Little is known about the mean surface drift directly south of the delta (Wiseman and Dinnel 1988).

Wright (1970) suggested that the tidal regime plays an important role in circulation at the mouth of South Pass. He found that the South Pass discharge "plume" turned more abruptly westward during flooding tide since the flood tidal wave travels from east to west. Generally, however, tidal currents are relatively weak in this region averaging about 15 $cm \cdot s^{-1}$ (Murray 1972). Tides in the area are mainly diurnal and have an average range of 30 cm (Murray 1972). Semidiurnal effects appear in the tide only during times of equatorial tides when tidal ranges and currents are smallest.

METHODOLOGY

Satellite Data Overview

This study utilizes digital data acquired by the Advanced Very High Resolution Radiometer (AVHRR) of the NOAA environmental satellites. This satellite data type was chosen as the main data source for several reasons. It provides the best available temporal resolution, at least 4 scenes/day, which enables assessments of daily changes in plume morphology, under clear-sky conditions. The spatial resolution (1.1 km) and regional coverage are optimal for studying the surface morphology of the river plume and simultaneous circulation features seaward of the river mouths. These data have been archived daily since July 1988 by the Coastal Studies Institute's Earth Scan Laboratory. The AVHRR provides five channels of information, two in the visible (yielding information on suspended sediment concentrations) and three in the thermal infrared range (for computing sea surface temperatures). Table 1 shows the wavelength characteristics of these five channels.

Table 1. NOAA Advanced Very High Resolution Radiometer (AVHRR) Characteristics.

Channel	Wavelength (μm)	Spatial Resolution (km)	Swath Width (km)
1	0.58 - 0.68	1.1	2800
2	0.70 - 1.1	1.1	2800
3	3.5 - 3.9	1.1	2800
4	10.5 - 11.5	1.1	2800
5	11.5 - 12.5	1.1	2800

As this is the first comprehensive study of the Mississippi River plume using satellite data, a large geographic area was included in the analysis: 25° to 31° N latitude and 86° to 98° W longitude.

The Mississippi River plume is revealed very differently by the visible (reflectance) and thermal infrared (SST) channels. Reflectance information provides a quantitative means of defining the Mississippi River sediment plume, and, therefore, has been used as the primary source of information in this report. The main drawback to its use is that once the suspended sediment has dropped out of suspension, the plume is no longer detectable by the satellite sensor. In terms of SST, the plume is "seen" if the temperature of Mississippi River water is substantially different from that on the continental shelf. This is often the case during autumn and spring when river water is generally cooler than the ambient shelf waters, as it has originated further north. During mid-winter, however, the shelf waters are often of a similar temperature to Mississippi River water, making it more difficult to track river water on the shelf. The SST signal, however, can be very useful in defining the maximum spatial extent of the Mississippi River plume, and it has been used for that purpose in this study. The SST information is also useful for detecting water of Loop Current origin. Its usefulness, however, deteriorates in summer due to high atmospheric water vapor loads and weak or non-existent SST gradients on the shelf.

"Surface-Truth" Data Collection and Analysis

The visible channels of the AVHRR, when properly processed, can provide important information on surface suspended sediment distribution and variability. The sediment plume also provides information concerning the distribution of pollutants in the northern Gulf of Mexico, as many pollutants are carried on fine-grained river sediments. It is desirable to be able to relate the satellite radiance information to in-situ concentrations of suspended sediments and, for this reason, a field component was included in this project.

In April 1992, two field trips were undertaken via helicopter to the Mississippi River bird-foot delta area with the purpose of collecting "surface-truth" data on suspended sediment concentrations. The principal investigator and one assistant flew from Baton Rouge to the study area with a fuel stop at Venice on April 14 and 28. River discharge in April 1992 was 15,736 $m^3 \cdot s^{-1}$, somewhat higher than the average discharge of 14,000 $m^3 \cdot s^{-1}$, but less than discharge during average flood conditions. Although the discharge was relatively low for spring, the field experiments were undertaken as there was a high probability that cloudiness would increase with the onset of summer, reducing the quality of the satellite imagery.

The technique of sampling by helicopter enabled identification of distinct turbidity regimes, homogeneous over sufficiently large areas (> 1 x 1 km). Approximately twenty-five samples were obtained during each trip, in the vicinity of Southwest Pass, by lowering a 500 ml bottle from the helicopter to the sea surface. Care was taken not to cause disturbance on the water surface from rotor wash. We found it necessary to remain 25 to 30 meters from the surface for this reason. During the 1st trip, on April 14, a very distinct river/oceanic front was encountered on the south side of Southwest Pass within a few kilometers of the river mouth. Approximately 8 km south of the pass, waters of Loop Current origin were encountered. This water mass could be described as exceptionally clear, turquoise in color, and abounding with Sargassum weed. During the 2nd trip, on April 28, the plume was again fairly confined which facilitated sampling a range of turbidity regimes efficiently in a short period of time. In Figure 2, the sites sampled on 28 April are superimposed on the corresponding NOAA-11 satellite reflectance data obtained simultaneously at 1530 CST (2130 Zulu).

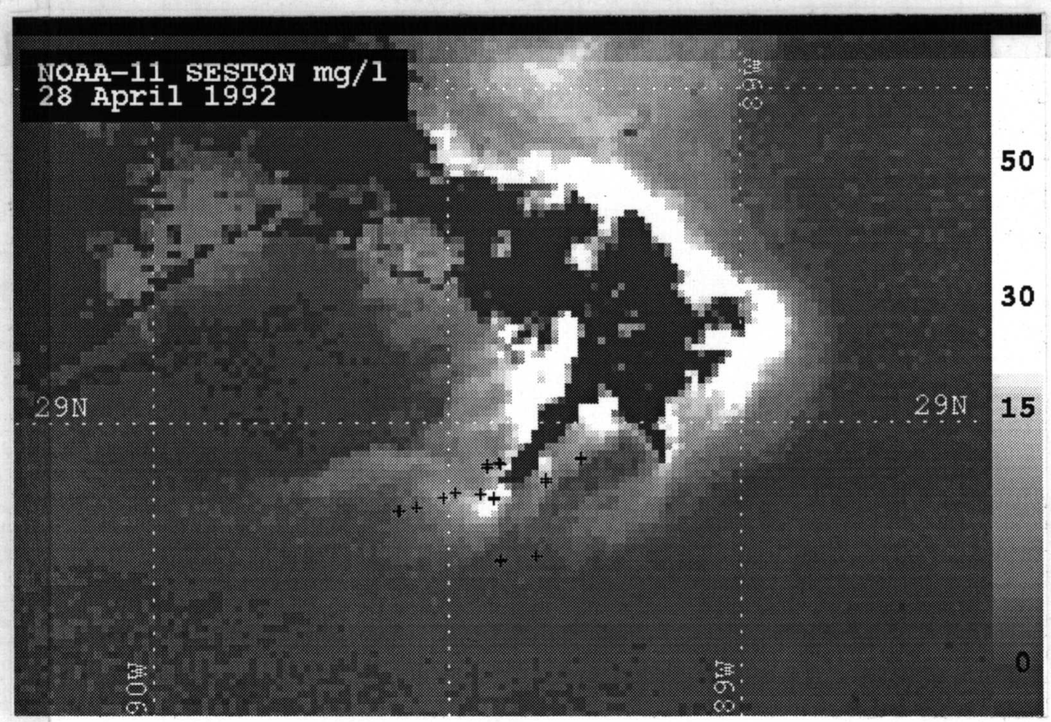

Figure 2. NOAA AVHRR reflectance data calibrated to suspended sediment concentration ($mg \cdot l^{-1}$) for 28 April 1992 (1530 CST). Sites sampled by helicopter at the time of image acquisition are depicted on the image with plus signs.

Seston is defined as the total suspended material which includes inorganic sediment, organic sediment and plankton. In this study, inorganic sediment dominated the seston concentrations and, thus, the terms suspended sediment and seston will be used interchangeably. Seston concentrations were determined by the glass-fiber filter method (U.S.Geological Survey 1987). Only the basic steps are repeated here. The 500 ml samples were filtered through 1.2 µm filters which had been previously dried and weighed. Each sample was carefully washed with distilled water to ensure that salt residue did not remain on the filter papers. Experiments with these filter papers revealed that, when properly washed, salt retention was much less of a problem than reported for the 0.47 µm filter papers (Trees 1978). Previous experimentation with Louisiana sediments indicated that >95% of sediments are retained when using 1.2 µm filters instead of the 0.47 μm filters. After filtering and washing, the filter papers were dried at 60°C for 12 hours and then reweighed. Concentrations of total suspended sediment, or seston, were calculated using the volume of each sample.

Suspended sediment concentrations were fairly low during each sampling trip, the highest value reaching 45 $mg \cdot l^{-1}$. In order to obtain a calibration algorithm which would be usable over a broader range of concentrations, additional field measurements overlapping with clear-sky imagery in the archive were sought. Suspended sediment concentrations were obtained from the Corps of Engineers for the Belle Chasse station, just south of New Orleans. Two data points were found which corresponded closely in time (within one day) with clear-sky imagery of the plume, and these two points were used in determining the final calibration algorithm.

Atmospheric Corrections of Satellite Radiance Data

In order to make comparisons of suspended sediment concentrations from image to image, it is necessary to perform certain atmospheric corrections to the satellite data to obtain water reflectances. The bias technique of Stumpf (1988, 1992) was implemented within our Terascan™ image processing software. A summary of the bias correction method is given below.

Water reflectance requires a correction for Rayleigh scattering, for aerosols, for the elevation of the sun, and for some transmission losses. The Rayleigh component does not change rapidly in the red and near infrared parts of the spectrum. Thus, when working in areas on the order of 200 km in the east-west direction, the Rayleigh component can be treated as a bias, simplifying the computation. Using this method, the water column reflectance R_d can be found from:

$$R_d \approx R_d' = R_c - R_{bias}$$

where:

$$R_c = \left[\frac{A(1)}{T_0(1)T_1(1)} - \frac{A(2)}{T_0(2)T_1(2)} \right] \quad (1 / r^2) * (1 / \cos\theta)$$

$A(\lambda)$ = albedo for channel λ, where $A = G * C + I$; G and I are calibration coefficients, and C = count value (0 - 1023)

$T_0(\lambda) = \exp\left[-(t_r(\lambda) / 2 + t_o(\lambda)) / \cos\theta \right]$

$T_1(\lambda) = \exp\left[-t_r(\lambda) / 2 + t_o(\lambda) \right]$

$(1/r^2) = [1 + 0.0167 \cos j]^2$ and $j = 2\pi (D - 3) / 365$; D is the Julian day

$\cos\theta$ = cosine of solar zenith angle at scene center
$t_r(\lambda)$ = Rayleigh optical depth for channel λ
$t_o(\lambda)$ = ozone and water vapor absorption optical depth for channel λ

and R_{bias} is the residual reflectance defined as R_c for a clear atmosphere over clear water near the area of interest.

For turbid water, reflectance can be approximated by the equation:

$$R_d' = (y * F) / (1 + G/n)$$

where n is the suspended sediment concentration in $mg{\cdot}l^{-1}$, y is 0.178, and

$F = b* / (b* + a*)$ where b* is the specific backscatter coefficient for sediment and a* is the absorption coefficient for sediment

$G = a_x / (b* + a*)$ where a_x is the absorption coefficient for non-sediment constituents.

From Stumpf (1988, 1992).

The equation was solved with the Newton method of non-linear curve-fitting using the suspended sediment concentrations obtained from the field sample analysis for 'n' and the satellite-derived reflectance values for 'R_d'. Figure 3 depicts the data points used to establish values for F and G in this study, the best-fit line and the 95% confidence limits. The root mean square error for this equation is 0.006. The coefficients obtained for the Mississippi River plume are similar to those obtained by Stumpf (1992) for Delaware Bay and Mobile Bay (Table 2).

Table 2. Coefficient comparisons.

Location	Satellite	F	G
Mississippi Plume (this study)	N-11	0.35	30.3
Delaware Bay (Stumpf 1992)	N-9	0.24	26.4
Mobile Bay (Stumpf 1992)	N-10/11	0.41	21.0

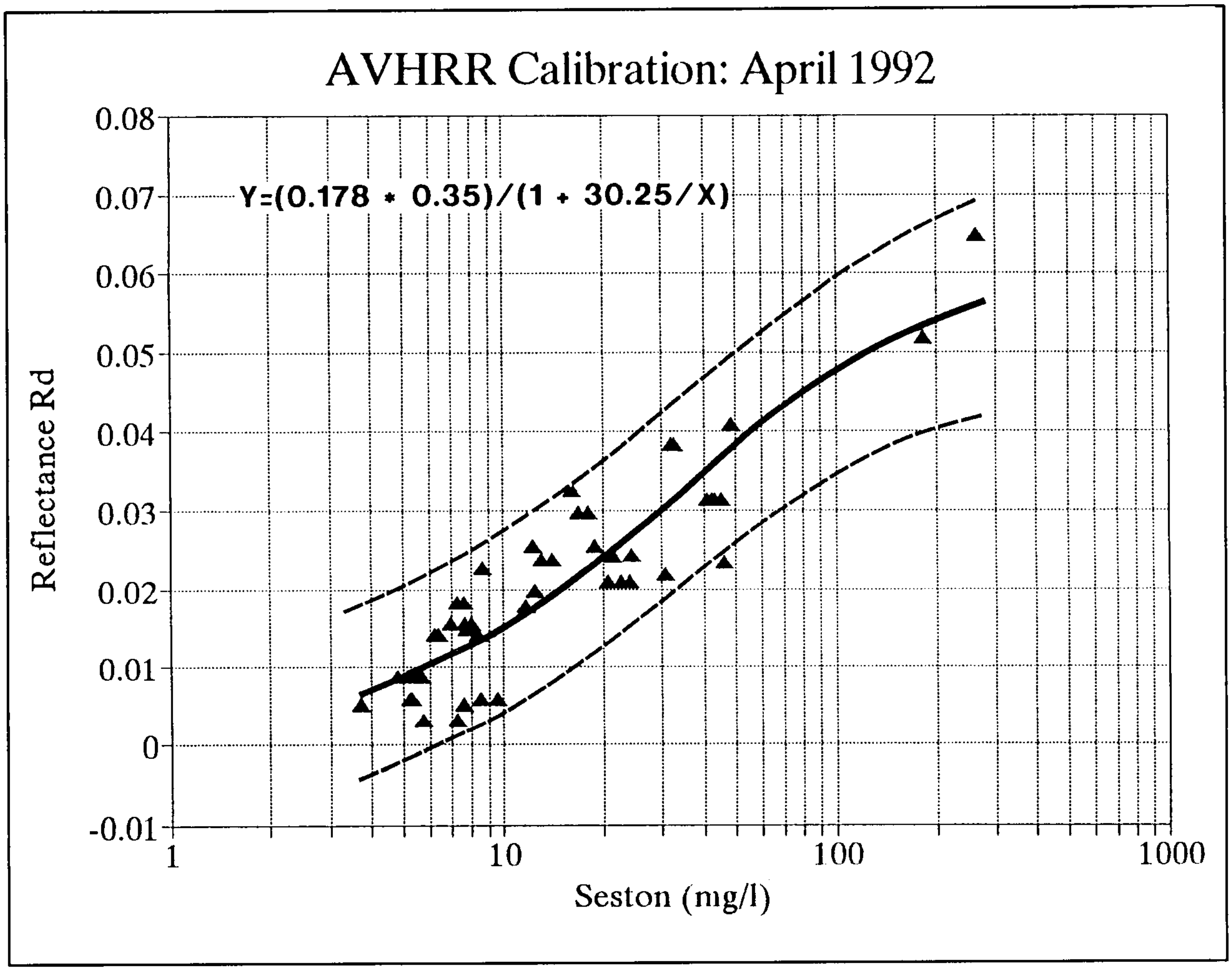

Figure 3. Suspended sediment concentration/AVHRR reflectance scatterplot and non-linear best fit equation.

Satellite Data Processing Procedures

At least two satellite images per day were uploaded from tape, calibrated and screened for cloud-cover during the time period from July 1988 through October 1992, yielding a total of 3000 images. Initially, cloud cover information from coastal weather stations was used in an attempt to reduce the amount of image processing to be performed. However, we found that the available coastal information did not adequately reflect cloud conditions over the northern Gulf of Mexico. Therefore, imagery was viewed for each day of the 4-year period. Satellite images of the Mississippi River plume or the northern Gulf of Mexico with less than 20% cloud-cover were saved for further processing. The additional processing steps included atmospheric correction for the retrieval of reflectance, calculation of SST, navigation and registration to a standard rectangular map projection. Sea surface temperatures were computed using the split-window multi-channel SST equations (McClain et al. 1985). The bias correction technique of Stumpf (1988, 1992) was used for the determination of reflectance. The processed satellite scenes were stored on 4 mm tapes for further screening by the principal investigator.

Daytime data obtained by the NOAA-11 satellite were used to investigate suspended sediment distribution. This satellite has been operational since mid-October 1988 and passes over the northern Gulf of Mexico about 2100 GMT (1500 CST) and 0900 GMT (0300 CST). In contrast to NOAA-9 and NOAA-10 which suffered from serious degradation of the visible sensors, NOAA-11 has shown near zero drift since launch (Y.J. Kaufman, NASA Goddard Space Flight Center, personal communication). The decision to restrict the sediment analysis to NOAA-11 data enabled a quantitative investigation into the distribution and variability of the Mississippi River sediment plume. Since the thermal infrared data is calibrated underway, it does not suffer from sensor degradation problems. The analysis of sea surface temperature patterns was, therefore, not constrained to one satellite. Table 3 presents a summary of clear-sky NOAA-11 daytime images available for analysis of which approximately 50% were used in this report. The method by which these were chosen is discussed in the Results section.

The final step in the processing of the satellite image data was to determine the spatial extent of turbid water on the continental shelf. This was accomplished by digitizing the sediment plume along a given isoline. The 10 and 30 $mg \cdot l^{-1}$ isolines were used. Results from both of these analyses are discussed in the Results section. The plume was divided into a western and eastern area by extending a line south from South Pass. It was also necessary to set a western limit for the western plume near the coast, to exclude sediments discharged from Barataria Bay. A northern limit was defined for the eastern plume area to exclude sediment resuspended in Chandeleur-Breton Sound. Statistics were compiled for the two areas separately and together. The procedure used in the satellite data processing is summarized in Figure 4.

Table 3. NOAA-11 daytime clear-sky image summary. Asterisks denote the months from which images used in the analysis were obtained.

	1988	1989	1990	1991	1992
JAN		-	8*	2	2*
FEB		4	6	2	2*
MAR		5*	5*	1	1*
APR		6*	5*	-	5*
MAY		5	3	1	5*
JUN		2	2*	2	1
JUL		2	4*	4	6
AUG		3	1	1	2
SEP	2	4	4	2*	4
OCT	3	12*	10*	5*	4*
NOV	3	4	12	2	
DEC	1	0	3	3	

Ancillary Data

Daily estimates of river discharge for the Mississippi River at Tarbert Landing and the Atchafalaya River at Simmesport were obtained from the U.S. Army Corps of Engineers, New Orleans District. In addition, suspended sediment concentration information within the Mississippi River was obtained from the Corps of Engineers and the United States Geological Survey, Baton Rouge Office. These data were used to select the time periods of investigation. They were also used in the regression analyses, after compensating for time-lags between Tarbert Landing and the Mississippi River mouths.

Hourly measurements of wind speed and direction at Grand Isle, Louisiana, were obtained from the National Oceanographic Data Center for the period January 1988 through December 1992 and were made available to the project free of charge by Dr. William Wiseman. The National Data Buoy Center in Slidell provided data for the period January 1992 through April 1992. Grand Isle is a barrier island located at the entrance to Barataria Bay, approximately one-third of the distance between the Mississippi and Atchafalaya plumes.

Tidal information was obtained from the NOAA Tide Tables, U.S. Department of Commerce.

Calibration of Visible and Thermal Channel Data
from count values to science units

↓

Initial Screening of Data for Cloud Cover

↓

Calculation of Sea Surface Temperature

↓

Navigation/Registration of Image to Standard Map Projection

↓

Secondary Screening of Data for Quality

↓

Atmospheric Correction of Visible Data to Reflectance

↓

Extraction of Statistical Information

Figure 4. Summary of satellite data processing steps.

RESULTS

Pilot Study of Sediment Plume/River Discharge Relationships

This preliminary study investigated whether river discharge is an important controlling factor for the distribution of surface river water and sediments on the continental shelf. In this analysis, variability of the Mississippi and Atchafalaya River plumes was studied during two months of the "high" discharge spring of 1989 (1 March - 30 April) and the "low" discharge spring of 1992 (29 February - 28 April) (Walker et al. 1992). Mean river discharges during the 1992 period were approximately one-half of those experienced in 1989. Eleven NOAA-11 daytime satellite images were used in the analysis. The sediment plumes were defined as those areas where suspended sediment concentrations exceeded 30 $mg \cdot l^{-1}$. Satellite data were displayed on the screen, contoured and digitized using Terascan™ software.

The application of linear regression techniques to the data revealed a strong relationship (r^2 = 0.83) between Mississippi River discharge and the areal extent of its sediment plume (Figure 5a). Mississippi River discharge ranged from a minimum of 11,643 $m^3 \cdot s^{-1}$ in 1992 to a maximum of 32,040 $m^3 \cdot s^{-1}$ in 1989. Associated plume areas varied by an order-of-magnitude, from 200 km^2 to 4014 km^2 (Table 4). In contrast to the Mississippi River plume results, a very weak relationship (r^2 = 0.29) was found between Atchafalaya River discharge and the area of its sediment plume (Figure 5b). Atchafalaya River discharge ranged from a minimum of 5,042 $m^3 \cdot s^{-1}$ in the 1992 spring to a maximum of 13,683 $m^3 \cdot s^{-1}$ in the 1989 spring. Atchafalaya plume areas varied from 240 km^2 to 2555 km^2 (Table 4).

Table 4. River discharge and plume areas for the Mississippi and Atchafalaya Pilot Study.

Day	Time	Mississippi River Discharge ($m^3 \cdot s^{-1}$)	Mississippi River Plume Area (km^2)	Atchafalaya River Discharge ($m^3 \cdot s^{-1}$)	Atchafalaya River Plume Area (km^2)
09 Mar 89	1851	31331	2290	13626	2555
13 Mar 89	1953	32040	4014	13683	1715
17 Mar 89	1911	31643	3536	13626	1843
01 Apr 89	2000	25326	1221	10708	2462
06 Apr 89	1908	24504	1695	10680	1887
24 Apr 89	1925	27195	2409	11615	958
29 Feb 92	2049	13116	766	6034	1981
15 Mar 92	2112	17563	946	7564	1613
14 Apr 92	2016	17903	908	6601	417
22 Apr 92	2016	12238	296	5071	1501
28 Apr 92	2050	11643	200	5042	240

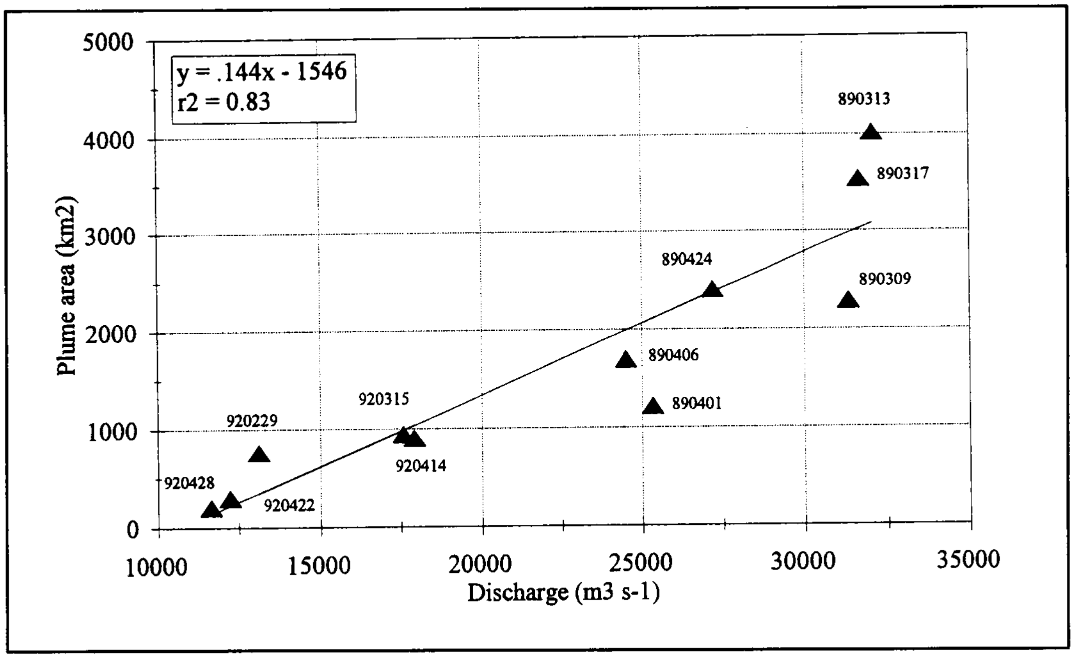

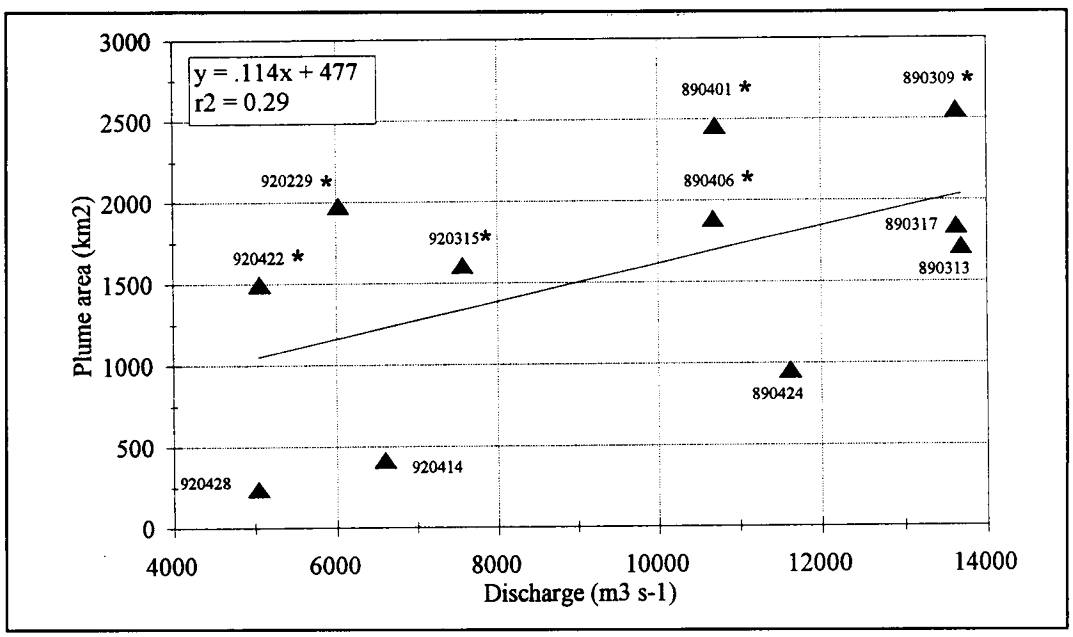

Figure 5. Relationship between river discharge and plume area for the a) Mississippi and b) Atchafalaya Rivers. The best-fit linear regression line, equation, and r^2 value are depicted. Image dates are shown in Year/Month/Day format (890313 represents 13 March 1989). In b, asterisks indicate image dates associated with strong winds (>6 m·s^{-1}).

The distinct differences observed between responses of the Mississippi and Atchafalaya River plumes to changes in discharge can be explained in terms of the bathymetry of their respective receiving basins. Atchafalaya Bay is extremely shallow (< 2 meters deep, except within the dredged navigation channel). The inner shelf, seaward of Atchafalaya Bay, is also shallow and shoaling as a result of the continual input of new sediments. For example, the 5 meter bathymetric contour lies 18 km seaward of the entrance to Atchafalaya Bay. Because of the shallow depths, much of the observed Atchafalaya "plume" was probably not newly discharged sediment, but sediment resuspended from the bottom by wind waves. The sites and degree of resuspension would have depended upon wind direction, speed, and fetch. Thus, the tremendous scatter observable in the Atchafalaya data is partially explainable in terms of variations in wind speed and direction prior to image acquisition. In Figure 5b asterisks denote wind speeds in excess of 6 $m \cdot s^{-1}$. It is noteworthy that the larger plume areas occurred when the wind exceeded the 6 $m \cdot s^{-1}$ cutoff. This suggests that resuspension and, also, sediment transport along and across the shelf under the influence of the wind increased the plume area measurements substantially. In contrast to the Atchafalaya, the Mississippi River is discharging, via several passes, into a relatively deep water environment and, thus, the plume consisted mainly of newly discharged river sediments with much less of a contribution from resuspended material.

Descriptive Map of the Mississippi River Sediment Plume

From January 1988 through December 1992, Mississippi River discharge exhibited order-of-magnitude fluctuations on the annual cycle with peak discharged occurring between January and June and lowest flow occurring from August through October (Figure 6). During this time period, the interannual variability of river discharge varied by a factor of two, considerably less variability than that exhibited by the annual cycle. The pilot study showed, however, that discharge variations of this magnitude (factor of two) can produce order-of-magnitude changes in the size of the Mississippi River sediment plume. During the study period, 1988 and 1992 were relatively low discharge years, falling below the 1950 to 1985 average discharge rate of 14,000 $m^3 \cdot s^{-1}$ (Table 5). The years of 1989, 1990, and 1991 exhibited water discharge well above this long-term average value.

Table 5. Annual mean Mississippi River discharge at Tarbert landing.

Year	Mean Discharge ($m^3 \cdot s^{-1}$)
1988	10622
1989	16222
1990	17404
1991	18330
1992	13269

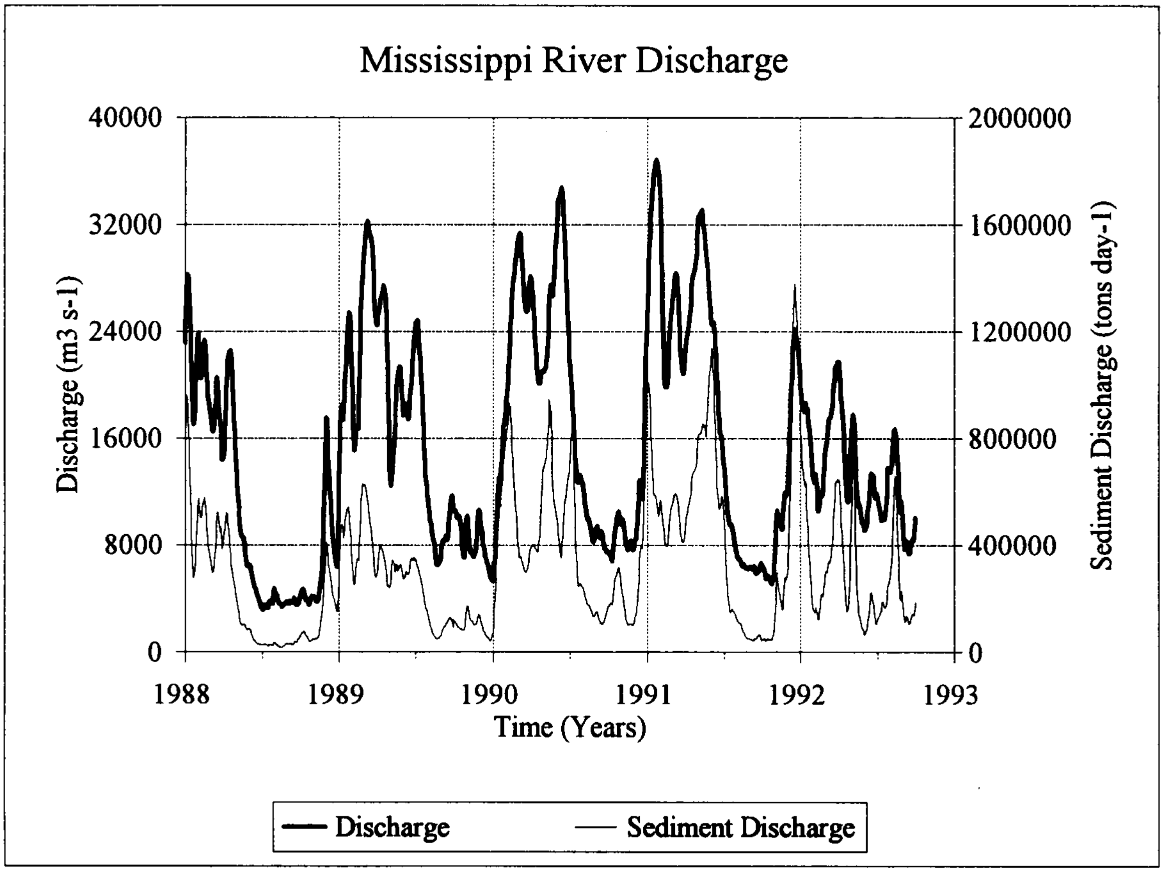

Figure 6. Mississippi River water and sediment discharge from January 1988 through October 1992.

Since the pilot study revealed the existence of a strong positive relationship between the area of the Mississippi River sediment plume and river discharge, further analyses of plume variability were based on this preliminary result. The forty-eight months between November 1988 and October 1992 were ranked according to mean water discharge (Table 6). This dataset was then divided into terciles; with low, medium, and high categories. Using the clear-sky satellite image compilation (Table 3) and the discharge information (Table 6), the best image months were chosen representing the entire range of discharge conditions from 5761 $m^3 \cdot s^{-1}$ (October 1991) to 33,561 $m^3 \cdot s^{-1}$ (January 1991). Eighty-three images from seventeen months were used in the final data analysis and interpretation. A more liberal definition of the plume was used in the final analysis. The sediment plume was defined as areas where surface suspended sediment concentrations exceeded 10 $mg \cdot l^{-1}$. Table 7 gives information on river discharge and plume areas for each image analyzed. The plume was divided into an eastern and western area by extending a line from South Pass to the southeast. Plume areas obtained from individual images revealed that plume size varied from 450 km^2 to 7700 km^2 (Table 7).

Table 6. Monthly mean Mississippi River discharges at Tarbert Landing: November 1988-October 1992.

Month	Mean Water Discharge (m3/s)	Month	Mean Water Discharge (m3/s)
Oct-91	5761	Mar-92	18734
Nov-88	6173	Jun-89	19243
Sep-91	6264	Jul-89	19859
Aug-91	6677	Feb-89	19975
Dec-89	7370	Dec-91	20210
Oct -92	7634	Jan-89	20399
Sep-92	8200	Jun-91	20802
Aug-89	8399	Apr-90	22909
Nov-89	8423	Feb-91	24145
Nov-90	8530	Mar-91	24866
Sep-90	8566	Feb-90	25146
Oct-90	8609	Apr-89	25295
Oct-89	9314	May-90	25299
Sep-89	9315	Apr-91	26528
Aug-90	10062	Mar-90	28177
Nov-91	10133	Mar-89	30070
Jul-91	10491	May-91	30780
Dec-88	10690	Jun-90	31433
Jul-92	11215	Jan-91	33561
Jun-92	11513		
Jan-90	11933		
Feb-92	12282		
Dec-90	12933		
May-92	12933		
Aug-92	13693		
Apr-92	15736		
Jul-90	16056		
May-89	17281		
Jan-92	17508		

Table 7. River discharge and plume areas for each satellite image used in the analysis.

IMAGE (YRMODA)	DISCHARGE LEVEL	WATER DISCHARGE (M3 S-1)	WEST AREA (KM2)	EAST AREA (KM2)	TOTAL AREA (KM2)
890309	HIGH	31076	3228	1582	4810
890313	HIGH	32040	3031	4668	7699
890314	HIGH	32040	1957	3229	5186
890317	HIGH	32040	3530	1747	5277
890330	HIGH	28243	3188	1930	5118
890401	HIGH	26006	1792	1207	2999
890404	HIGH	24873	1505	2196	3701
890406	HIGH	24504	1258	1306	2564
890408	HIGH	24788	1194	1920	3115
890416	HIGH	26487	2446	1158	3603
890424	HIGH	27195	1977	2197	4175
891001	MEDIUM	11728	1543	1930	3473
891002	MEDIUM	11416	1242	1368	2610
891003	MEDIUM	11190	1140	829	1969
891005	MEDIUM	10680	834	1012	1846
891020	MEDIUM	10085	1506	1744	3251
891023	LOW	9065	584	728	1312
891024	LOW	8499	394	567	961
891025	LOW	8074	606	554	1160
891027	LOW	7422	400	1042	1442
891028	LOW	7138	584	1222	1807
891029	LOW	7082	1223	1288	2511
891030	LOW	7167	503	1252	1756
900101	LOW	5524	1572	1398	2970
900109	LOW	6713	1004	1074	2078
900111	LOW	6912	1635	1302	2938
900112	LOW	7564	1625	1107	2732
900114	LOW	9121	1699	1405	3104
900115	MEDIUM	10142	1758	1320	3078
900126	MEDIUM	14278	2313	1645	3959
900131	MEDIUM	16997	3161	1331	4493
900317	HIGH	28187	3137	1633	4770
900318	HIGH	27904	3213	1904	5116
900321	HIGH	26600	1867	1905	3772
900323	HIGH	25750	2246	1684	3931
900326	HIGH	25496	3283	1444	4727
900403	HIGH	27904	2449	1130	3579
900405	HIGH	28159	2205	2466	4671
900411	HIGH	26062	2246	1310	3557
900421	HIGH	20765	1488	1444	2932
900429	HIGH	20567	758	1339	2097
900604	HIGH	31785	2889	2830	5719

IMAGE (YRMODA)	DISCHARGE LEVEL	WATER DISCHARGE (M3 S-1)	WEST AREA (KM2)	EAST AREA (KM2)	TOTAL AREA (KM2)
900612	HIGH	34221	5938	NA	NA
900703	HIGH	24193	1515	2373	3888
900707	HIGH	21643	3212	938	4150
900725	MEDIUM	12748	761	287	1049
900731	MEDIUM	13173	616	494	1110
901012	LOW	7252	433	790	1223
901013	LOW	7223	397	638	1035
901014	LOW	6969	756	902	1658
901015	LOW	6799	695	769	1464
901025	LOW	9490	1071	1255	2325
901026	LOW	9688	1090	1614	2704
901027	MEDIUM	10028	815	1390	2205
901028	MEDIUM	10198	647	1250	1897
901030	MEDIUM	10538	424	685	1109
901031	MEDIUM	10368	383	769	1152
910912	LOW	6261	266	184	450
910927	LOW	6033	289	1177	1466
911011	LOW	6204	631	519	1150
911012	LOW	6034	967	606	1573
911016	LOW	5524	550	994	1544
911017	LOW	5524	266	449	715
911019	LOW	5807	376	500	876
920103	HIGH	21416	3144	1865	5008
920120	MEDIUM	18499	3886	2064	5950
920207	MEDIUM	12833	3874	1969	5843
920229	MEDIUM	12805	1237	1547	2784
920315	MEDIUM	17564	716	1396	2112
920414	MEDIUM	18159	1137	1232	2369
920421	MEDIUM	13144	1504	759	2263
920422	MEDIUM	12748	1056	572	1629
920427	MEDIUM	11246	512	876	1388
920428	MEDIUM	11331	392	1017	1409
920506	MEDIUM	16912	406	785	1191
920513	MEDIUM	16317	1326	708	2034
920514	MEDIUM	15439	629	543	1172
920516	MEDIUM	13654	592	502	1094
920524	MEDIUM	11048	478	344	822
921004	MEDIUM	10057	2549	2325	4875
921012	LOW	9858	1043	1239	2282
921013	LOW	9405	913	1196	2108
921014	LOW	9235	736	1174	1910

Since river flow can vary greatly even within a month, as revealed by Figure 6, the satellite images were grouped according to river discharge into the following categories: 0 - 10,000; 10,001 - 20,000; and 20,001 - 35,000 $m^3 \cdot s^{-1}$. Plume are statistics were compiled according to discharge level (Table 8). It is clearly seen that the mean plume area increased with increasing river discharge in both the eastern and western plume areas. The standard deviation of the mean, however, was very high. It is interesting to note that under low flow conditions, the mean plume area in the east was slightly larger than that in the west, but as discharge increased, the western plume area became larger. Possible explanations for this result will be discussed later.

Table 8. Plume area statistics compiled according to river discharge level.

Discharge ($m^3 \cdot s^{-1}$)	Images	Western Area (km^2)		Eastern Area (km^2)		Total Area (km^2)	
		mean	$	mean	$	mean	$
0 - 10,000	28	797	440	962	360	1759	726
10,001-20,000	29	1291	987	1127	550	2418	1432
20,001-35,000	26	2488	1053	1896	797	4312	1200

Descriptive maps of the Mississippi River sediment plume were compiled according to discharge variations. In Figure 7, the spatial distribution of Mississippi River surface sediments on the continental shelf and slope during low discharge conditions is depicted. The map was produced as follows. The twenty-eight images within the low discharge category (Table 8) were composited to reveal the minimum pixel value, the mean pixel value and the maximum pixel value within each image group. This technique was also used to investigate sediment distribution patterns for images of the medium and high discharge categories (Figures 8 and 9).

Under low discharge conditions, the maximum "composite" plume extended 20 km offshore to the 100 meter contour, 50 km west of Southwest Pass and 20 km east of Pass a Loutre (Figure 7). The eastern plume extended 50 km northeast from Cubits Gap and Main Pass. The area of the maximum "composite" plume for the low discharge image group was 4,239 km^2 and the area of the mean plume was 1,804 km^2. The minimum "composite" plume covered 171 km^2 and was primarily on the east side. The sediments observed on the east side of the delta in the minimum plume analysis may have resulted from resuspension by prevailing easterly wind-generated waves.

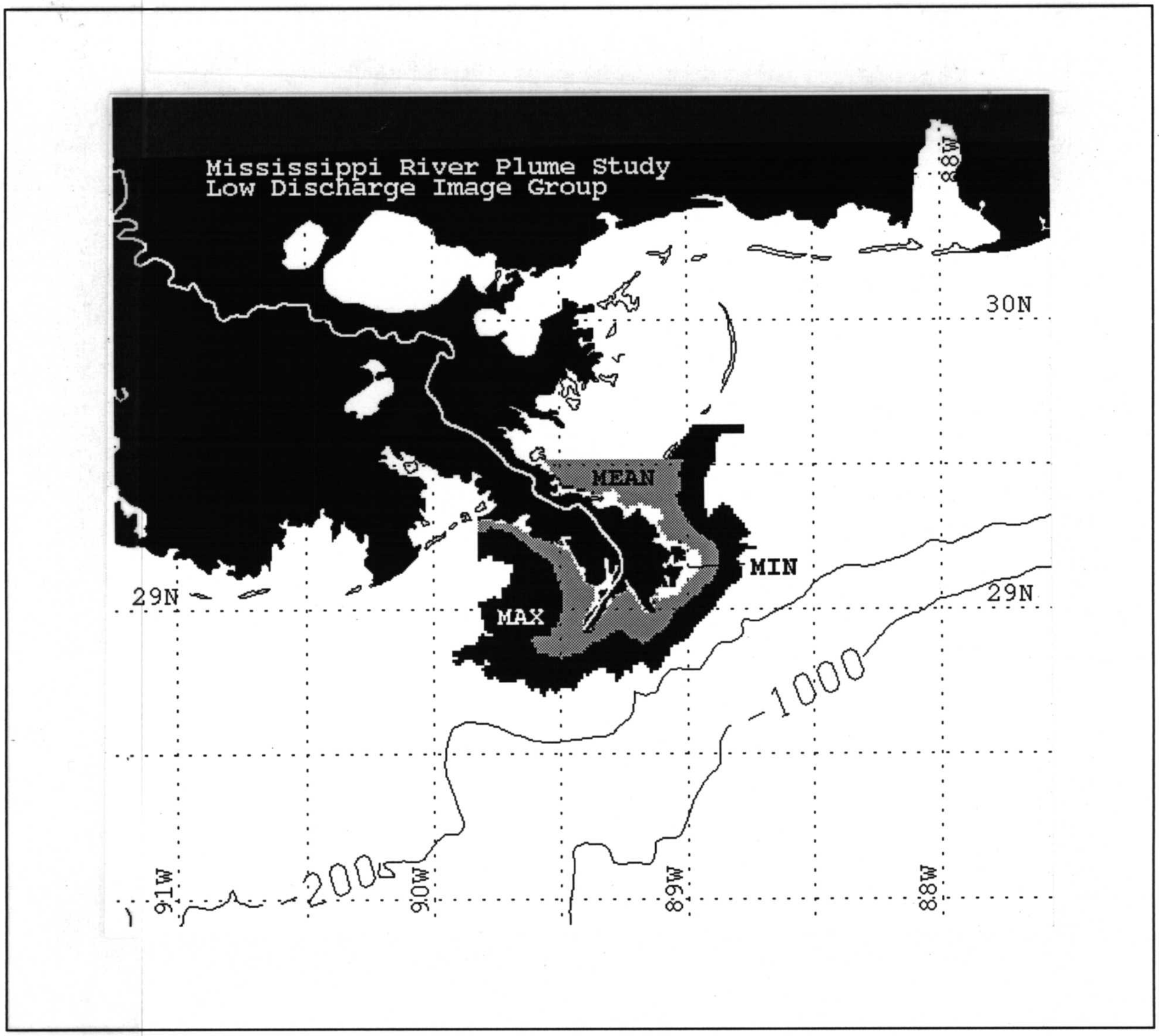

Figure 7. Mississippi River sediment plume composite map for the low river discharge image group. The minimum, mean, and maximum plumes are displayed with gray shades ranging from white to black.

Under medium discharge conditions, the maximum "composite" plume was double the size of the maximum plume under low discharge conditions. It exhibited a distinct southwest-northeast orientation, with a total areal extent of 8,130 km² (Figure 8, Table 9). The sediment plume extended about 90 km toward the southwest following the 200 meter contour closely until encountering the Mississippi Canyon region west of 89° 30' W, where it flowed over the continental slope. It extended about 60 km towards the northeast from Pass a Loutre. The mean plume, of 2,165 km², was only 20% larger than that of the low discharge image group. The minimum "composite" plume was an order of magnitude smaller than the mean plume, covering 227 km².

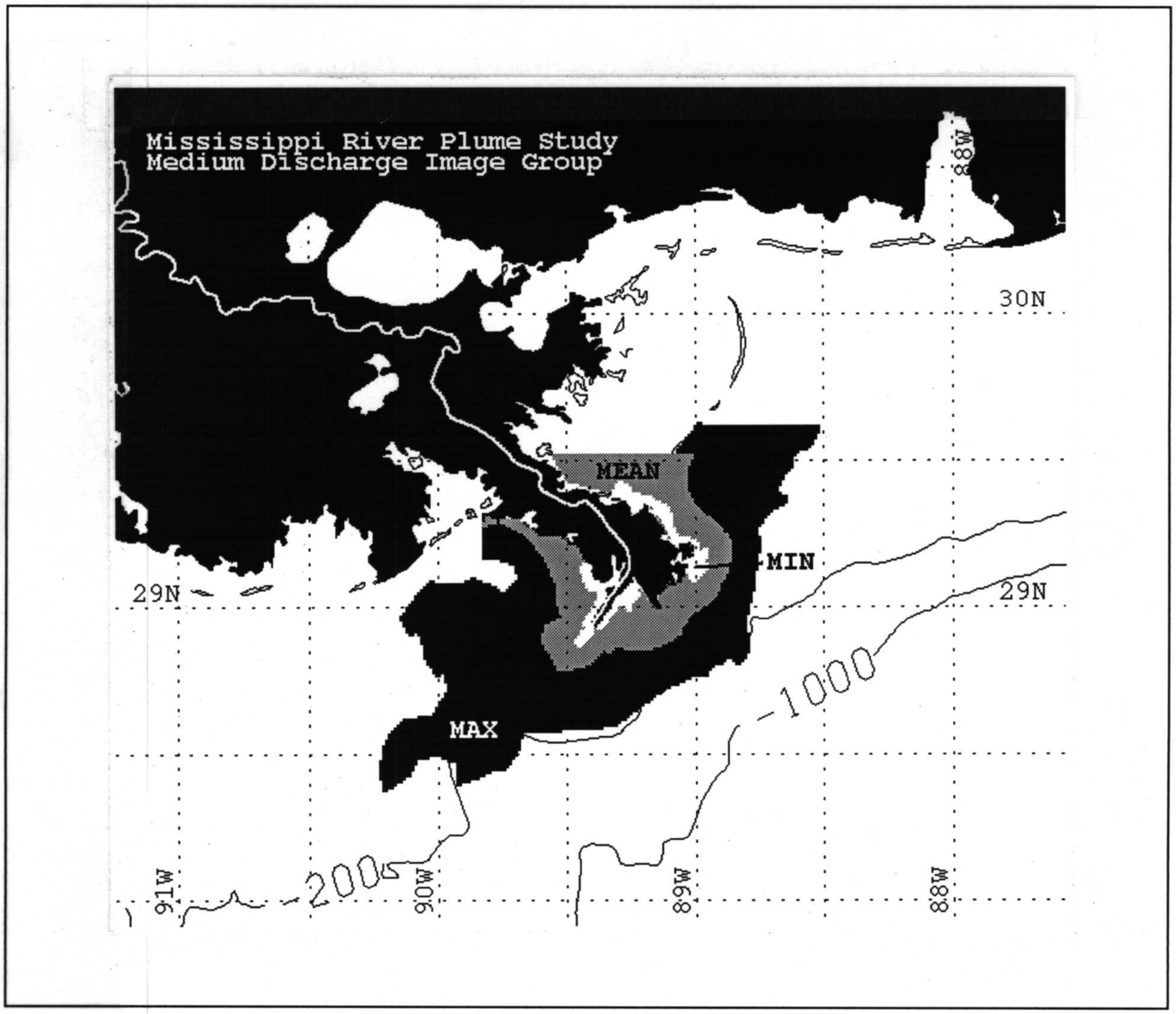

Figure 8. Mississippi River sediment plume composite map for the medium river discharge image group. The minimum, mean, and maximum plumes are displayed with gray shades ranging from white to black.

Under high discharge conditions, the maximum "composite" plume covered an enormous area of the continental shelf and slope totaling 13,207 km^2 (Figure 9, Table 9). It extended 80 km southward to the 1000 m isobath, 125 km west of Southwest Pass, and about 60 km northeast of Pass a Loutre. The mean "composite" plume covered 3,909 km^2, double that of the medium discharge group. It extended slightly seaward of the 100m isobath in a southerly direction. The minimum plume covered 944 km^2 with somewhat more area in the east and south than in the west. Again, the effects of wind-wave sediment resuspension could explain this result.

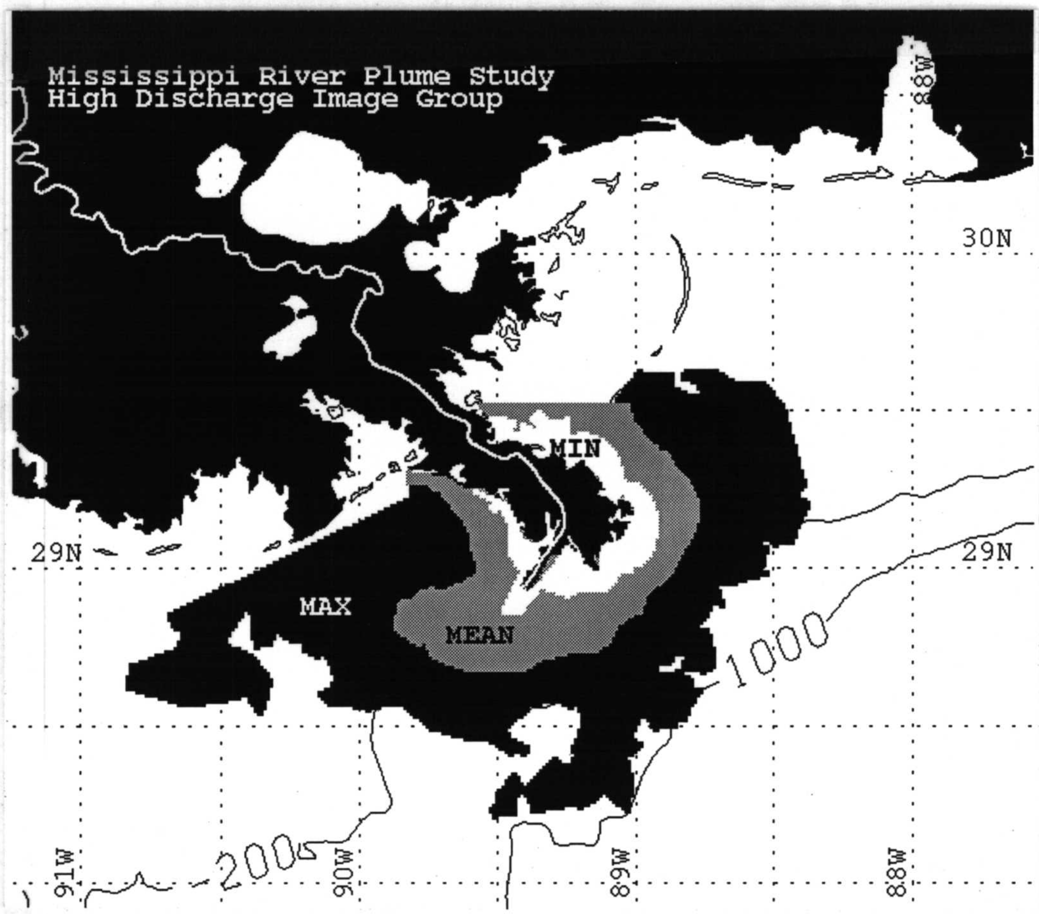

Figure 9. Mississippi River sediment plume composite map for the high river discharge image group. The minimum, mean, and maximum plumes are displayed with gray shades ranging from white to black.

Table 9. Mississippi River plume area statistics from the compositing analysis, where seston concentrations exceeded 10 $mg \cdot l^{-1}$.

Discharge ($m^3 \cdot s^{-1}$)	Minimum (km^2)	Mean (km^2)	Maximum (km^2)
0 - 10,000	171	1804	4239
10,001 - 20,000	227	2165	8130
20,001 - 34,220	944	3909	13207

Forcing Mechanisms for Plume Variability

It is beyond the scope of this one year study to undertake a detailed statistical analysis of the forcing mechanisms for plume variability, however, certain relationships have become clear in the course of this investigation which will be discussed in this section. Linear regression was used to investigate the relationships between plume area and river discharge variations for the eastern, western, and total plume area. Figure 10 shows the scatterplot and best-fit linear equation for the western plume area and river discharge. The image dates are displayed using an abbreviated Year/Month/Day format. For example February 7, 1992 is represented by 920207.

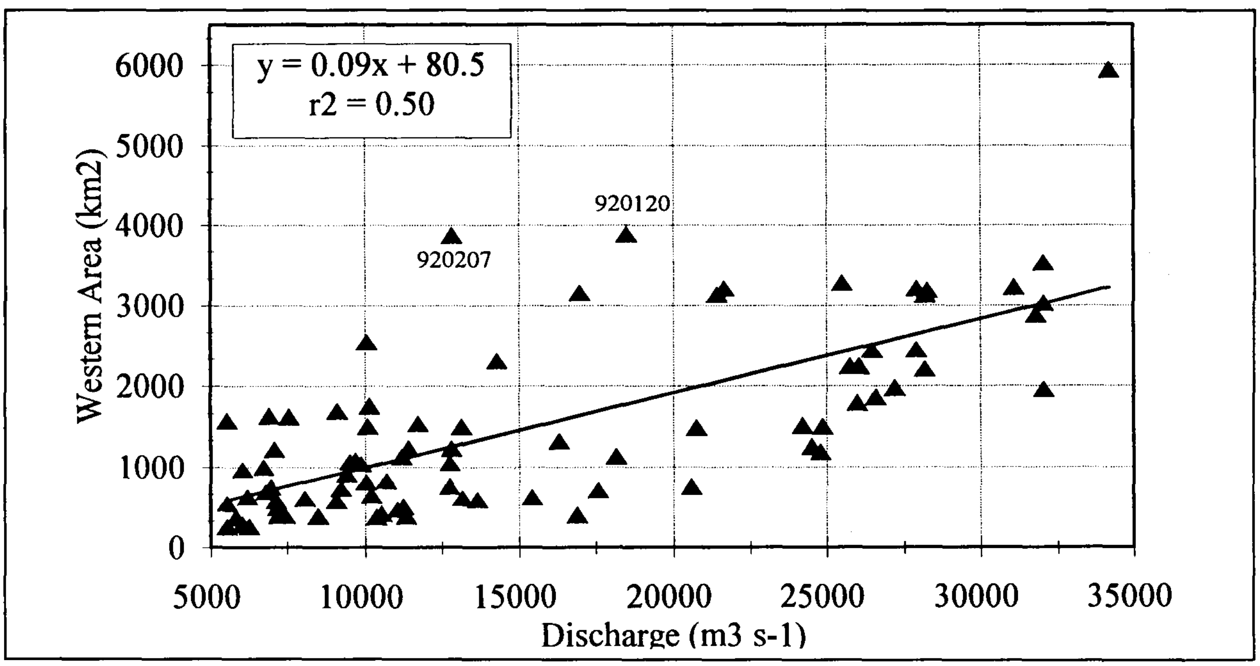

Figure 10. Relationship between river discharge and plume area west of South Pass. Individual images referred to in the text are labeled using the Year/Month/Day format.

A positive relationship (r^2 = 0.50 with 81 degrees of freedom) was determined, however, a tremendous amount of scatter was revealed by the analysis.

A similar analysis was performed for the eastern area (Figure 11), and an even weaker relationship was found (r^2 = 0.30). Although the standard deviations about the mean were consistently lower for the eastern area (Table 8), the line was very flat and a six-fold increase in discharge resulted in only a doubling of the plume area. For the western area, a six-fold increase in the discharge resulted in a six-fold increase in plume area.

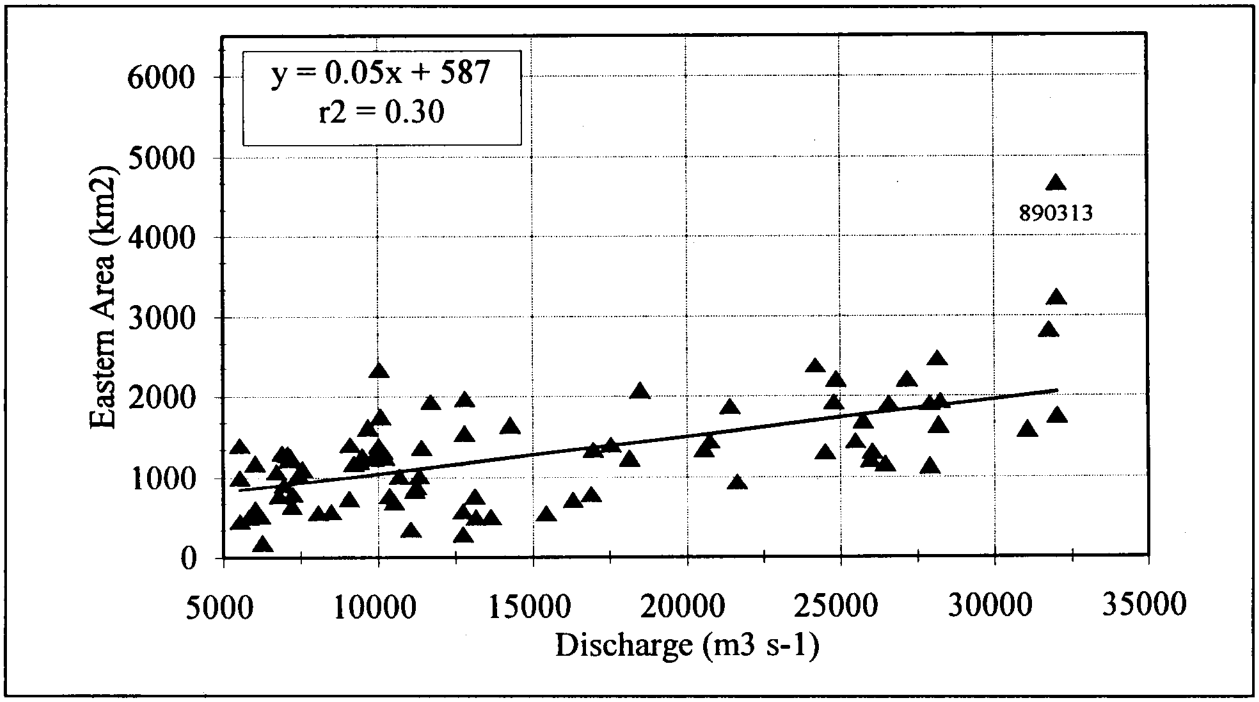

Figure 11. Relationship between river discharge and plume area east of South Pass. The images referred to in the text are labeled using the Year/Month/Day format.

The highest positive correlation ($r^2 = 0.56$) was found using the total plume area in the analysis (Figure 12).

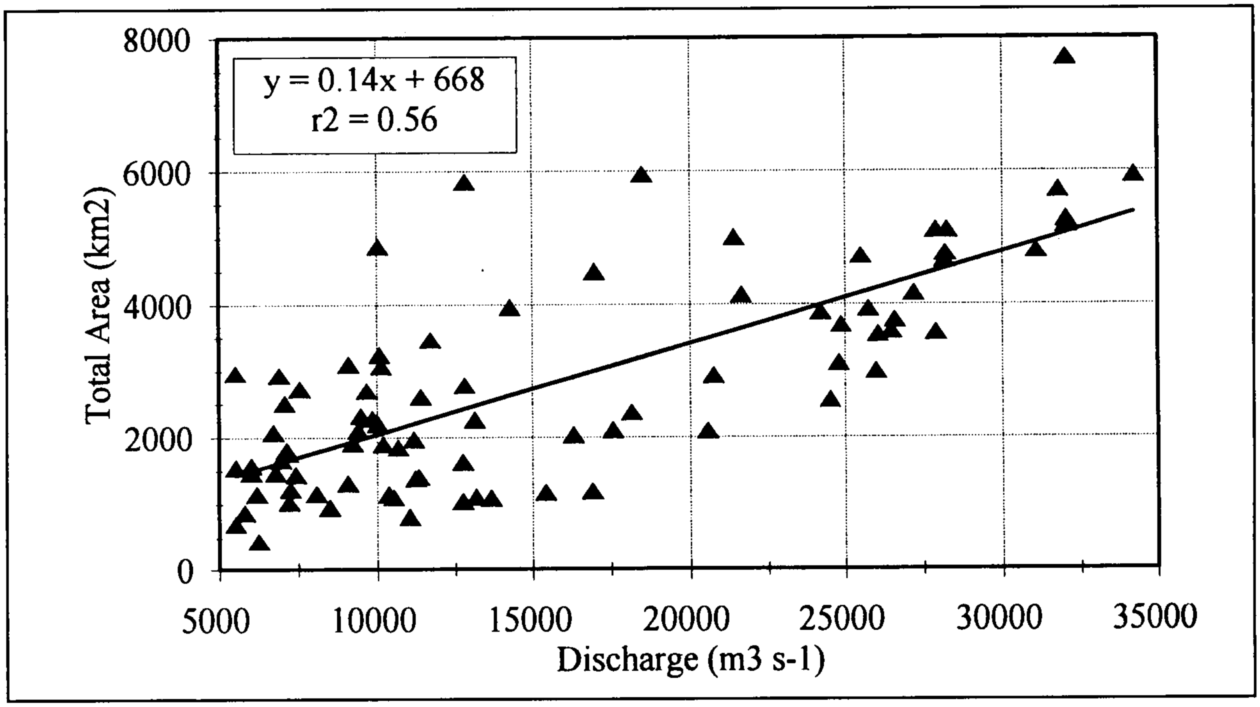

Figure 12. Relationship between river discharge and total plume area.

These results differ substantially from those of the pilot study where a much better correlation was obtained between river discharge and plume area ($r^2 = 0.83$). This difference probably results from the use of a more liberal definition of the plume in the present analysis (10 $mg \cdot l^{-1}$ in this study as opposed to 30 $mg \cdot l^{-1}$ in the pilot study). Regression analyses similar to the above were performed using sediment discharge data (Figure 6) rather than water discharge measurements. The relationships between river discharge and plume areas were found to be much weaker using the sediment discharge information.

The size of the sediment plume on the eastern side of the delta was only weakly associated with discharge variations. A few explanations are proposed for these results. As the prevailing wind direction along the Louisiana coast is easterly, the eastern delta area is more frequently subjected to wind-waves and sediment resuspension processes. In addition, the area to the east of the delta is shallower than the areas to the south or west (Wright and Coleman 1974). Thus, the sediment "plume" east of the delta is probably comprised of resuspended sediments as well as newly discharged sediments, analogous to the Atchafalaya results in the pilot study. In addition, the prevailing easterly wind regime would tend to inhibit the transport of sediment and river water to the east confining it to a nearshore plume. A close examination of the SST information revealed that detached Loop Current filaments and eddies are often situated near the 200 meter contour of up on the shelf east and southeast of the delta, further inhibiting the eastward flow of sediment-laden water. Essentially, the existence of semi-permanent convergence zones east and southeast of the delta would confine the sediment and freshwater plume closer to the coast on the east side of the delta than on the west side. All of these factors could contribute to the weak correlation identified in this analysis between river discharge and plume size on the east and southeast sides of the delta. There was evidence from the sediment distribution maps, composited from low and medium discharge images, that a portion of the sediment emanating from passes on the east side of the delta moves northeastward toward the Mississippi and Alabama coastline (Figures 7,8). Under conditions of high wind speeds, however, it is difficult to identify Mississippi river sediments from those which may have exited Chandeleur-Breton Sound.

A closer examination of the discharge/plume relationship for the western area (Figure 10) reveals that wind forcing was a critical factor in determining plume size and orientation. In Figure 10, plume areas which were larger than predicted by the best-fit line were found to occur in association with strong wind events, usually from a northerly or westerly direction. The satellite images of 20 January 1992 and 7 February 1992 will be discussed in terms of wind forcing and sediment transport process. Grand Isle wind data revealed that both of these images were obtained just after passage of winter cold fronts, which brought strong and sustained northerly winds to the area. Strong northeasterly winds preceded the 20 January 1992 image and strong northwesterly winds preceded the image of 7 February 1992.

The 20 January 1992 images (Figure 13) were obtained after two days of persistent northeasterly winds with speeds ranging from 8 to 18 $m \cdot s^{-1}$ at Grand Isle. The distribution of suspended sediment (seston) observed on 20 January 1992 is shown in Figure 13a. River water and sediments were clearly moving towards the southwest along the southern side of the delta where the sediment-laden water was confined to the continental shelf (< 200 m). The plume was deflected northwestward towards the coast in the vicinity of the Mississippi River Canyon, near 89°50'W (A, Figure 13a). Upon encountering the coast between Barataria Bay and Terrebonne Bay, the plume was deflected to the west (B, Figure 13a). Near 91°W, the Mississippi and Atchafalaya sediment plumes appeared to merge into a giant plume covering a large portion of the shelf west of the Balize delta. The strong northeasterly winds had resuspended a substantial amount of sediment in shallow areas of the inner shelf seaward of Atchafalaya Bay and the Atchafalaya plume (C, Figure 13a) covered an extensive area of the continental shelf. The Atchafalaya plume probably inhibited further westward movement of the Mississippi plume.

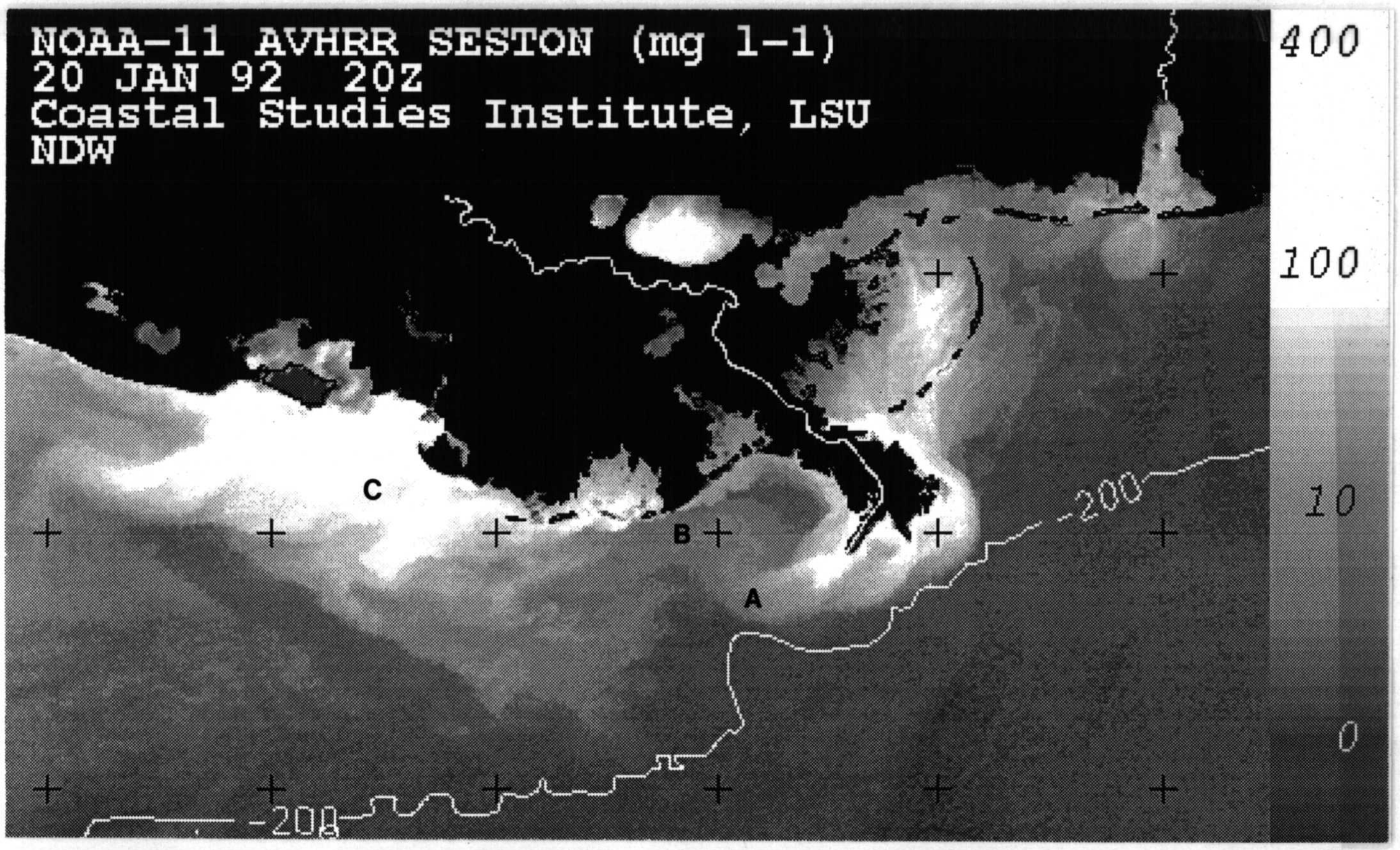

Figure 13. a) NOAA-11 AVHRR satellite image obtained on 20 January 1992 (2000 Z) (processed to reveal seston concentration in $mg{\cdot}l^{-1}$).

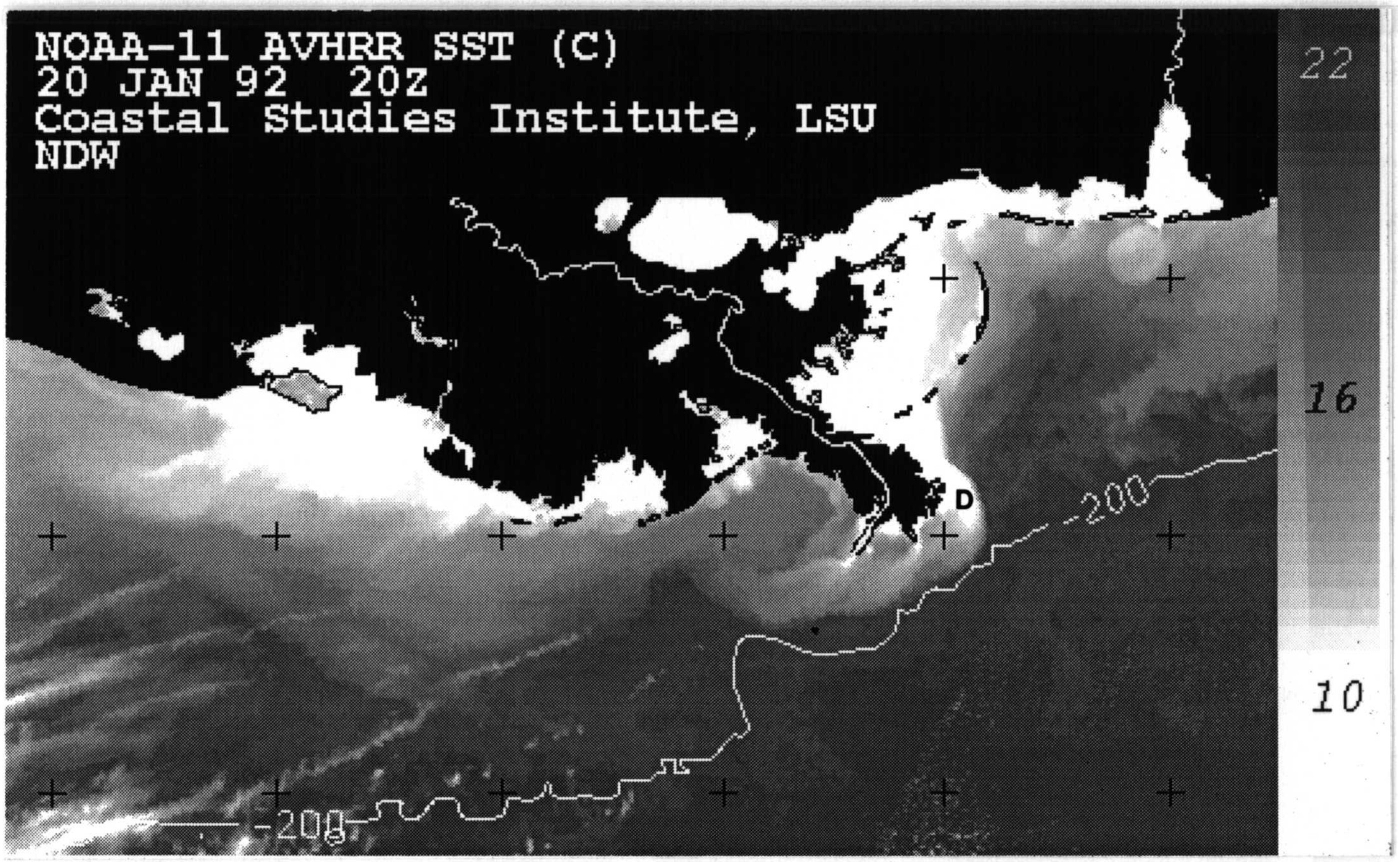

Figure 13. b) NOAA-11 AVHRR satellite image obtained on 20 January 1992 (2000 Z) (processed to reveal sea surface temperatures in degrees Celsius).

On a smaller scale, the individual sediment plumes emanating from Southwest Pass and South Pass were distinct (Figure 13). East of the delta, the highest concentration of sediment increased in a southerly direction suggesting that water had moved southward and turned anticyclonically towards the west before encountering the 100m contour. The strongest gradients in suspended sediment concentration were observed east and southeast of the plume suggesting the existence of strong convergence of water masses. The corresponding SST image revealed a tongue of cooler water extending from the east side of the delta around the delta front to the west (D, Figure 13b). Such a flow is consistent with the suggestion of Schroeder et al (1985) that southward flow along the east side of the delta can be initiated by northeasterly winds associated with cold front passages.

Northwesterly winds of 6 to 14 $m \cdot s^{-1}$ (at Grand Isle) were experienced for two days prior to acquisition of the 7 February image. East of the delta, sediment-laden water was forced southward and a sizable mini-plume was observed extending south-southwest to the 200 m contour (A, Figure 14). The sediment-laden water exiting Southwest Pass and further north along the west side of the delta was observed to move primarily to the southwest towards the northern margin of the Mississippi River canyon (B, Figure 14). A high concentration of sediment covered the continental shelf south of the Balize delta. Two sites of off-shelf flow of river water were observed, one extending southeastward from the Mississippi Canyon region (C, Figure 14) and the other extending southeastward from the east side of the delta (D, Figure 14). This off-shelf flow was most likely initiated by the strong northwesterly wind forcing. The more western plume feature turned abruptly to the east after crossing the 1000 meter contour (E, Figure 14). Both sediment-laden flows crossed the 2000 meter isobath, a distance of 150 km from the Balize delta.

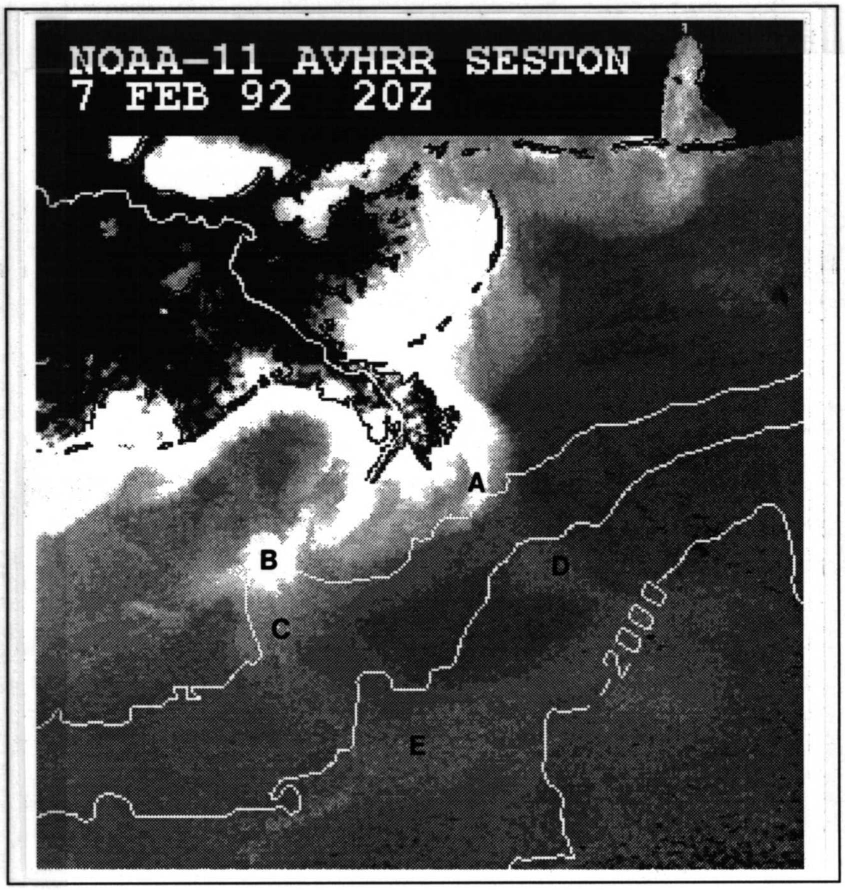

Figure 14. NOAA-11 AVHRR satellite image obtained on 7 February 1992 (2000 Z) (processed to reveal seston concentrations).

A close inspection of the river/discharge relationship for the east area reveals that the plume of 13 March 1989 was abnormally large in comparison with all other data points (Figure 11). Moderate southwesterly winds (6-7 $m \cdot s^{-1}$) prevailed at Grand Isle for 48 hours prior to image acquisition. Wind speeds may have been even stronger offshore. A distinct anticyclonic circulation was observed west of the delta within the Louisiana Bight in both the seston image (A, Figure 15a) and the SST image (A, Figure 15b). Abnormally high concentrations of suspended sediments were observed east of the delta, most likely as a result of the prevalence of southwesterly winds for the preceding 2 days (B, Figure 15a). In addition, a narrow band of turbid water was observed to extend almost due south from the east side of the delta seaward to the 2000 m contour (C, Figure 15a). The corresponding SST image revealed the existence of a Loop filament east of this feature (D, Figure 15b) which probably had a major affect on the offshore advection of the sediment-laden plume water. The westerly wind regime probably initiated the off-shelf movement of plume water, whereas the Loop feature may have had a more dominant influence on its motion seaward of the 200 meter isobath.

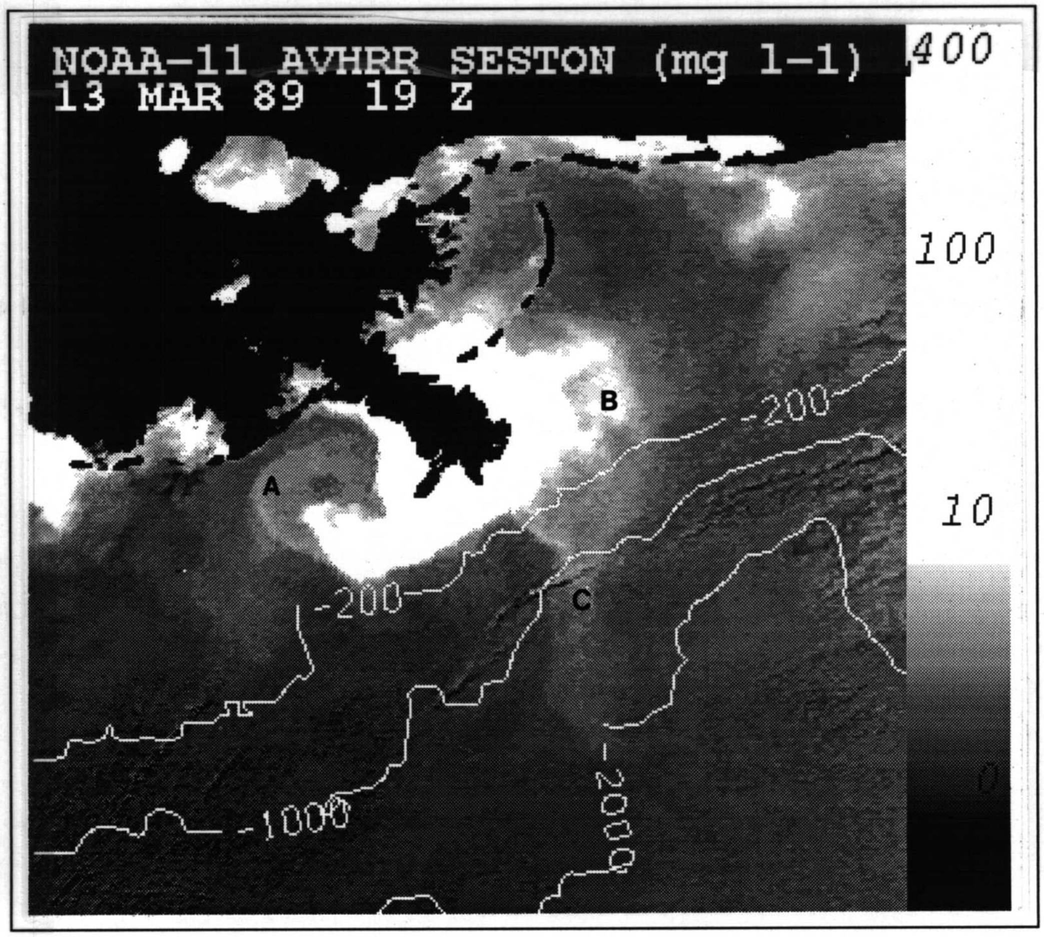

Figure 15. a) NOAA-11 satellite image obtained on 13 March 1989 (1900 Z) (processed to reveal seston concentrations in $mg \cdot l^{-1}$).

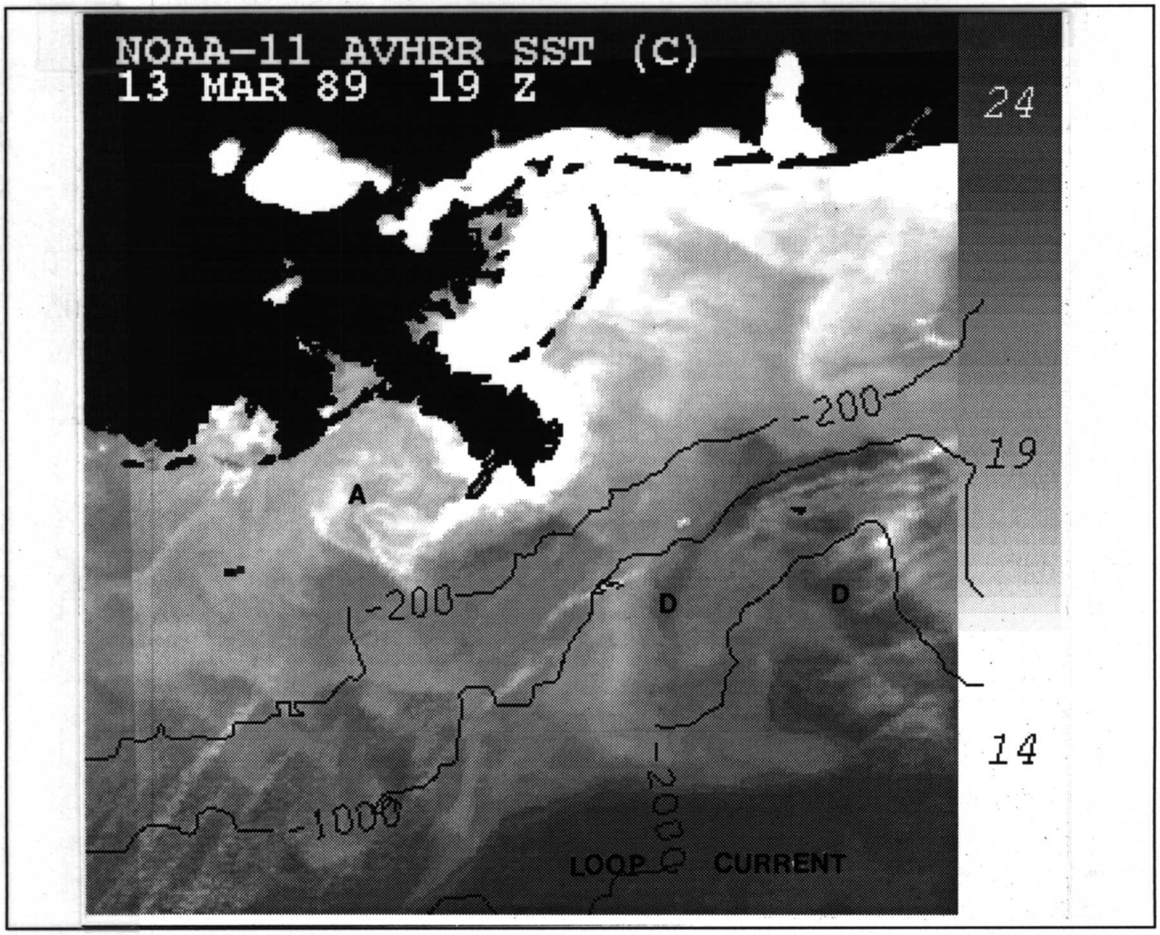

Figure 15. b) NOAA-11 satellite image obtained on 13 March 1989 (1900 Z) (processed to reveal sea surface temperatures in degrees Celsius).

A Case Study of Abnormal Shelf Circulation: October 1992

Since wind has been identified as a major forcing agent for sediment transport, it is relevant to investigate an unusually strong wind event which occurred in early October 1992 during which a sequence of cloud-free images revealed abnormal circulations associated with Mississippi River water. From September 30 through October 3, strong northeasterly winds between 10 and 18 $m \cdot s^{-1}$ were experienced in the vicinity of the Mississippi River delta. The strongest winds (15-18 $m \cdot s^{-1}$) occurred on October 2 and 3 and resulted from a tropical depression which moved north from the Yucatan region into the northern Gulf of Mexico. A strong pressure gradient developed between a high pressure system over the east coast and this low pressure system. Exceptionally strong and sustained northeasterly winds blew along the northern Gulf of Mexico coast.

The cumulative effects of the north-northeasterly wind forcing were readily observable in clear-sky imagery obtained during the first two weeks of October. A considerable amount of heat was lost to the atmosphere from the shallow inner shelf waters, particularly on the east side of the delta. These cold coastal waters in tandem with the relatively cold river water were "trackable" as a distinct plume using sea surface temperature (SST) information. In Figure 16, the primary SST fronts (obtained by use of a Sobel filter) from a series of satellite images are shown to illustrate the movement of an extensive cool water plume towards the southwest from the Mississippi delta region. On 4 October, the seaward margin of this cool feature followed the 200 meter bathymetric contour closely and a narrow "jet" of cool water (A, Figure 16a) was detected over the Mississippi Canyon region. A semi-submersible drilling platform situated in the canyon in 500 meters of water, owned by Ensearch Corporation (Dennis Cox, Ensearch Inc., personal communication), encountered severe difficulties due to exceptionally strong currents on October 2 through 4.

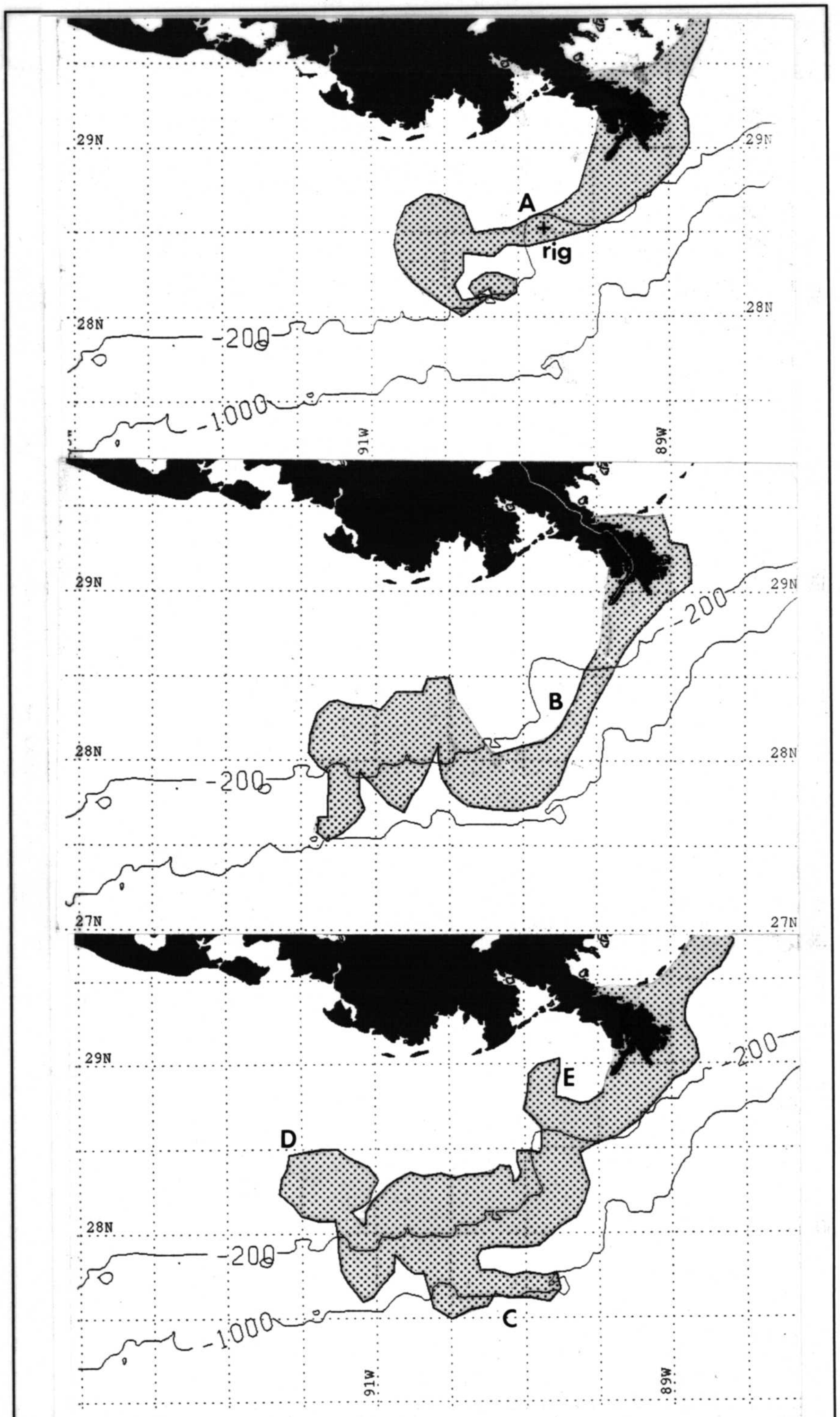

Figure 16. Primary SST fronts associated with the river/shelf water "plume" on a) 4 October 1992, b) 11 October 1992, and c) 13 October 1992.

After October 4, the plume continued to move towards the southwest, even though the easterly wind forcing between October 4 and October 11 had weakened substantially (< 8 $m \cdot s^{-1}$). By October 11, the "jet" of cool water (near the Mississippi Canyon) (B, Figure 16b) had taken a more southerly course, an observation not readily explainable by offshore wind events. Two days later on October 13 (Figure 16c) the narrow jet (south of the canyon) had been replaced by a wider, meandering plume which extended seaward beyond the 1000m isobath. One week after the initial disturbance, much of the cool water which originated in shallow areas east of the delta and within the river now covered the continental slope region and extended westward to 91° 25' (Figure 16c). By 13 October, a portion of the cool feature had been advected along the 1000 m contour by slope currents towards the east (C, Figure 16c) and a large mushroom-shaped feature (D, Figure 16c) had formed along the northwest margin of the cool plume, extending the plume even further westward to 91° 40' W. There was evidence of a newly formed river plume within the Louisiana Bight rotating in a clockwise direction (E, Figure 16c).

The circulation features observed on the shelf and slope regions were substantially effected by ocean circulation involving two large anticyclonic Loop Current eddies, Eddy Vasquez (A, Figure 17) and Unchained Eddy (B, Figure 17), which were rotating in the northwestern Gulf of Mexico. The SST image of 13 October 1992 clearly illustrates the two eddies and the cool inner shelf/river water (C, Figure 17) southwest of the bird-foot delta region. The large-scale circulation associated with the northern flanks of these eddies was eastward, opposite to the wind-driven westward flow. Circulation on the western side of the plume was strongly influenced by a convergence of water masses in the northwestern Gulf of Mexico between the 100 m and 1000 m contours. This convergence zone formed at the confluence of westward flow on the shelf and eastward flow associated with Eddy Vasquez over the slope and deeper Gulf. The westward flow of plume water was inhibited by this convergence and the interesting mushroom-shaped feature (perhaps an eddy-dipole) formed rapidly in a northwest direction as a result (D, Figure 17). A portion of the outer plume split off from the main "plume" and was advected between the two eddies with a maximum observed seaward extent of 27° N, 91° 30' W (not shown). These water mass movements are best observed by "animating" the clear-sky imagery, a capability of the Terascan™ image processing software.

This case study provides evidence that, under the influence of strong and sustained northeasterly wind forcing, shelf water can be rapidly forced away from the delta and onto the continental slope. Thus, wind-driven transport of the buoyant river water has been identified as the dominant mechanism controlling the offshelf movement of river water, sediments and pollutants. Detached Loop current eddies and filaments provide the major control on circulation of plume waters on the continental slope and in deeper parts of the northern Gulf of Mexico.

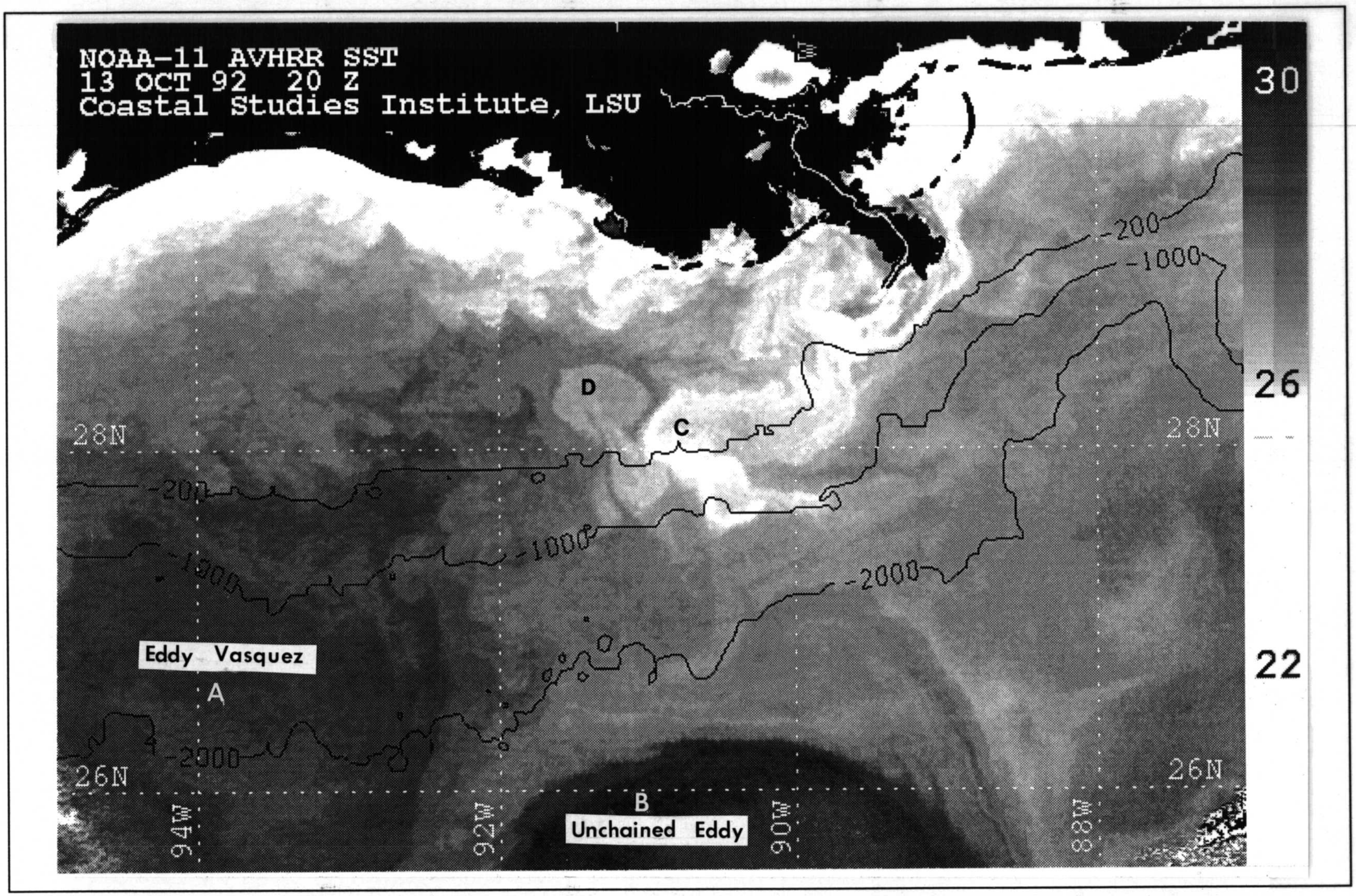

Figure 17. NOAA-11 AVHRR sea surface temperature image of 13 October 1992 (depicting the spatial extent of cool river/shelf waters on the continental shelf and slope southwest of the Mississippi delta).

DISCUSSION

The spatial structure of the Mississippi River sediment plume has been investigated in relation to river discharge. In general, the size of the sediment plume was found to be a function of river discharge, higher discharge generally yielding larger plumes. Detailed analysis of eighty-three satellite images revealed that the Mississippi sediment plume undergoes dramatic changes in areal extent and surface morphology on time scales of hours and days. The individual images revealed plume areas ranging from 450 km^2 under low discharge conditions to 7700 km^2 under high discharge conditions. Plume areas varied by as much as 2000 km^2 in 24 hours (Table 7). The size of sediment plumes in the western area (west of South Pass) was better correlated with river discharge variations. Figure 18 synthesizes information obtained through the compositing analyses presented in the Results section. It illustrates sediment plume distribution in the northern Gulf of Mexico under medium and high river discharge conditions.

The spatial distribution of the mean sediment plume under all discharge conditions indicates that most of the sediment emanating from the Mississippi River is trapped on the continental shelf. The smallest plume shown in Figure 18 is the mean plume under medium discharge conditions, 10,000 - 20,000 $m^3 \cdot s^{-1}$ (Figure 18, 'C'). It covered 2200 km^2 (Table 9) and was similar in size on the west and east sides of the delta (Table 8). The mean plume under high discharge conditions (Figure 18, 'B') was double the size of the mean plume under medium discharge conditions. Under high discharge conditions, the mean plume showed disproportionate enlargement towards the west and south, in comparison with the east. A number of factors may help explain these results. Sharp gradients in suspended sediment concentrations and sea surface temperatures were often observed on the eastern and southeastern sides of the plume, indicating the existence of strong surface convergence zones which would restrict the movement of river water towards the southeast and east and enhance sediment deposition in this region. This convergence zone could result from the prevailing easterly wind regime and also from the frequent intrusions of detached Loop Current filaments and eddies onto the continental slope and shelf in this region. Where the eastern plume did extend towards the east, its orientation was more northeastward and, at times, Mississippi sediments were transported into the Chandeleur-Breton Sound (Figure 8). It is also possible that, under conditions of high discharge, the prevailing westward flow around the delta becomes more efficient as the freshwater lens increases in size both vertically and horizontally. Alternatively, the percent flow through Southwest Pass and South Pass may increase under high discharge conditions. Field measurements would assist in confirming or rejecting these hypotheses.

The mean orientation of the sediment plume west of Southwest Pass (Figure 18, 'B') suggests the existence of a semi-permanent clockwise rotation of water and sediment at the surface into the Louisiana Bight. Such a circulation was reported previously by Wiseman et al. (1976) and Rouse and Coleman (1976). The satellite imagery revealed that flow generally exits Southwest Pass to the southwest, then recurves to the west and north into the Bight. A distinct anticyclonic (clockwise) rotating circulation pattern in the Louisiana Bight was observed in approximately 50% of the images analyzed. Its direction of rotation is consistent with that of an inertial current. This general clockwise rotation into the bight ensures that a substantial portion of the river's sediments, nutrients, and pollutants are trapped there. The sediment plume west of the delta was also observed to turn westward along the coast where its westward progress was soon impeded by the Atchafalaya plume. In some cases the sediment plume was seen "colliding" with the coastline between Barataria Bay and Terrebonne Bay before turning westward. The spatial distribution of hypoxic conditions west of the delta during summer (Rabalais et al. 1991) corresponds well with the often observed sediment distribution patterns revealed in individual satellite images.

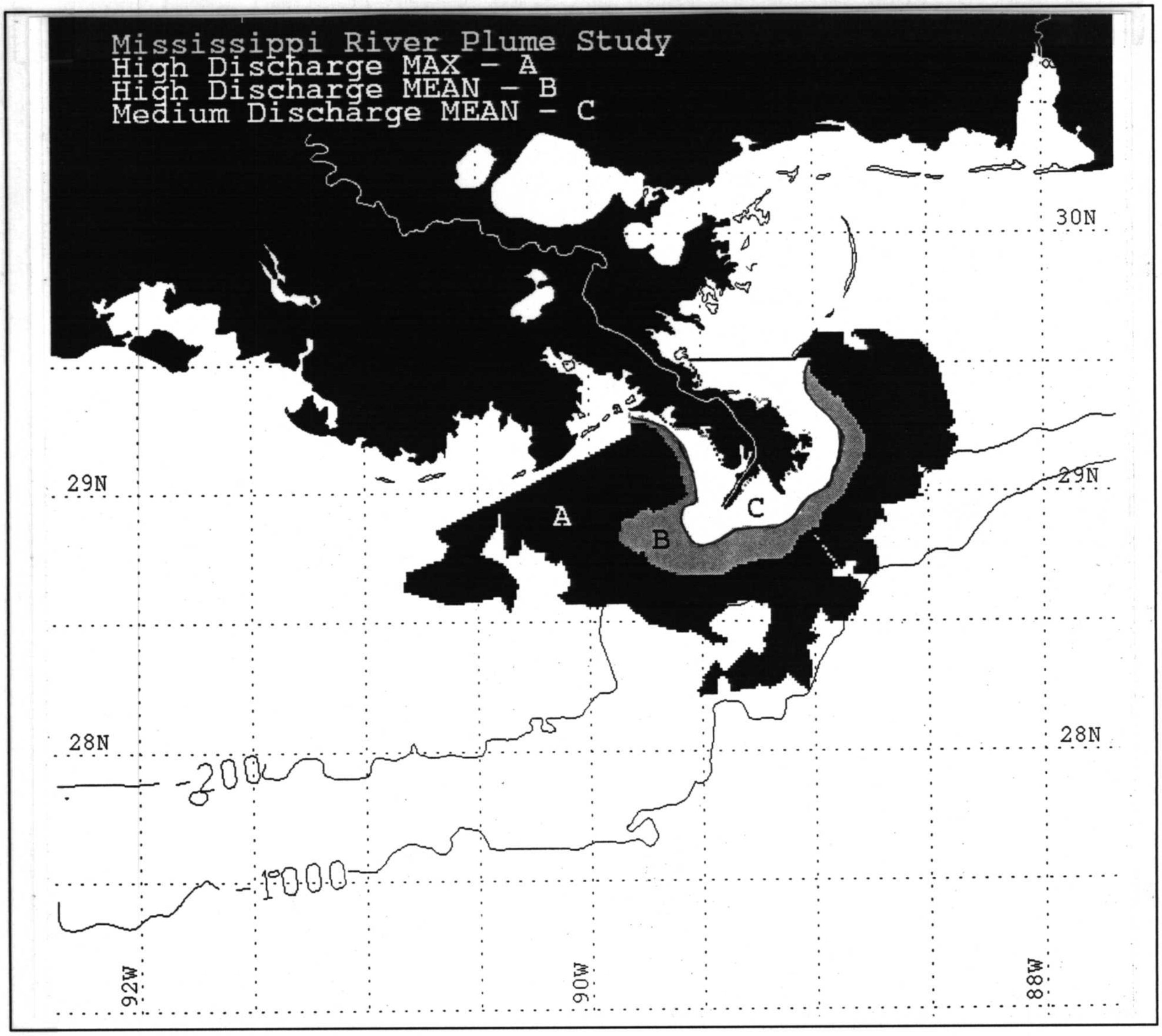

Figure 18. Mississippi River sediment plume composite map summary [depicting the mean plume under medium discharge conditions (C), the mean plume under high discharge conditions (B), and the maximum spatial extent of the sediment plume under high discharge conditions(A)].

Close inspection of the individual satellite images suggests that discharge from Pass a Loutre often flows south along the coastline and then westward, joining the South Pass discharge in its westward course. This observation is in agreement with the suggestion of Wright and Coleman (1974) that the zone of intermediate salinity water seaward of the South Pass plume originates from passes further east. This southward flow is best observed in winter in association with strong northeasterly winds, a process which was described by Schroeder et al. (1985). This process was revealed in the imagery of 20 January 1992 (Figure 13), 7 February 1992 (Figure 14) and the image set from 4 through 13 October 1992 (Figure 16). Thus, the satellite observations suggest that a substantial amount of river water discharged on the east side of the delta flows westward, under the appropriate wind conditions.

The maximum composite plume (Figure 18, 'A') covered an area of 13,207 km^2, over 3 times that of the mean plume (Table 9). It extended westward along the shelf for 125 km, southward to the 1000 meter isobath and northeastward about 60 km. The wide-ranging sediment distribution along the continental shelf and onto the continental slope is mainly a function of speed, direction and fetch of surface winds prior to image acquisition. Strong northeast winds resulted in maximum sediment transport to the west along the continental shelf, and under extreme conditions (i.e. October 4-13, 1992) river water flowed over the continental slope and into the deep Gulf. Sustained northwesterly winds most efficiently moved the western sediment plume off-shelf in a southerly and southeasterly direction. Westerly winds were also most efficient at moving sediments of the eastern portion of the plume eastward along the shelf and off-shelf towards the southeast. Thus, this study has demonstrated the critical role played by strong westerly and northerly winds (usually associated with cold-front passages) in initiating off-shelf movement of river water and sediments at least in the surface layer. This confirms the previous observations of Roberts et al. (1987) concerning the important effect of cold-front passages on sediment transport along the Louisiana coastline. Having flowed off of the continental shelf, the plume is then subjected to oceanic forcing, which in the northern Gulf of Mexico often involves circulation patterns associated with eddies and filaments, detached from the Loop Current. The large persistent Loop Current eddies rotate anticyclonically, however, cyclonic eddies are frequently observed east of the delta. Currents associated with these eddies and filaments can augment the off-shore movement of river water, particularly once the water has reached the continental slope (Figure 15).

CONCLUSIONS

The sediment "plume" of the Mississippi River influences an extensive area of the continental shelf and slope, extending from 88° 20' W to 90° 50' W, and, at times, covering an area in excess of 13,000 km^2. The gross characteristics of the Mississippi sediment plume are controlled by river discharge. However, extreme changes in size and surface morphology of the sediment plume can be attributed to strong wind events, often associated with cold-front passages in winter. Dramatic changes in plume orientation can occur in a matter of hours as a result of altered wind forcing.

Although the plume water and sediments were usually observed on the continental shelf, within the 200 meter isobath, substantial cross-shelf and shelf-slope exchanges of plume water were observed in association with strong wind events. Off-shelf movement of river water was maximized during and subsequent to the occurrence of sustained strong winds from the southwest, northwest and northeast. Westerly winds were found to be most efficient at forcing plume waters seaward. Having flowed off the continental shelf, the plume was then subjected to prevailing ocean currents often associated with detached Loop Current eddies and filaments. Satellite imagery revealed extreme excursions of Mississippi River water towards the south and southwest in excess of 150 km from the Balize delta. It should be pointed out that these results under-estimate the spatial extent of river waters within the Gulf of Mexico, since the sediment plume disappears once the sediment drops out of suspension and the river's temperature will change over time through air-sea interactions.

This satellite-based assessment of the Mississippi River plume has suggested that the proportion of water flowing westward increases during winter and possibly also under high discharge conditions. Under the influence of strong northeasterly winds, river water from the eastern passes and ambient coastal waters flow southward hugging the eastern delta region. They subsequently turn westward to join the discharge emanating from South Pass and Southwest Pass. To the west of the Balize delta, the shelf circulation is generally anticyclonic (clockwise) within the Louisiana Bight although a portion of the plume often flows further westward. The net result is an accumulation of river sediments, pollutants and nutrients within the Bight and on the continental shelf west of Southwest Pass.

This investigation has revealed that river discharge, wind forcing, and shelf currents are the major factors controlling the distribution of Mississippi River water, sediments, and pollutants on the continental shelf. Significant off-shelf transport of plume waters occurs only in association with strong northerly or westerly winds. Subsequently, the movement of river water over the continental slope and deep Gulf is controlled mainly by ocean currents, often associated with Loop Current eddies and filaments.

LITERATURE CITED

Chew, F., K.L. Drennan and W.J. Demoran. 1962. Some results of drift bottle studies off the Mississippi Delta. Limnol. Oceanogr. 7:252-257.

Cochrane, J.D. and F.J. Kelley. 1986. Low-frequency circulation on the Texas-Louisiana continental shelf. Journal of Geophysical Research. 91(C9):10,645-10,659.

Dagg, M.J. and T.E. Whitledge. 1991. Concentrations of copepod nauplii associated with the nutrient rich plume of the Mississippi River. Continental Shelf Research. 11(11):1409-1423.

Dagg, M.J., P.B. Ortner, and F. Al-Yamani. 1987. Winter-time distribution and abundance of copepod nauplii in the northern Gulf of Mexico. Fishery Bulletin. 86:319-330.

Dinnel, S.P. and W.J. Wiseman, Jr. 1986. Fresh water on the Louisiana and Texas shelf. Continental Shelf Research. 6(6): 765-784.

Dinnel, S.P., W.W. Schroeder, and W.J. Wiseman, Jr. 1990. Estuarine-shelf exchange using Landsat images of discharge plumes. Journal of Coastal Research. 6(4):789-799.

Ebbesmeyer, C.C., G.N. Williams, R.C. Hamilton, C.E. Abbott, B.C. Collipp, and C.F. McFarlane. 1982. Strong persistent currents observed at depth off the Mississippi River delta. Proc 14th Int. Offshore Tech. Conf. Houston, Texas. pp 259-267.

Fernandez-Partegas, J. and C.N.K. Mooers. 1975. Some front characteristics over the eastern Gulf of Mexico and surrounding land areas. Final report to the Bureau of Land Management under contract 08550-CT4-L6.

Fisk, H.N., E. Mc Farlan, C.R. Kolb, and L.J. Wilbert. 1954. Sedimentary framework of the modern Mississippi delta. J. Sedimentary. V 24.

Gagliardini, D.A., H. Karszenbaum, R. Legeckis, and V. Klemas. 1984. Application of Landsat MSS, NOAA/TIROS AVHRR, and Nimbus CZCS to study the La Plata River and its interaction with the ocean. Remote Sensing of Environment. 15:21-36.

Huh, O.K. and K. J. Schaudt. 1990. Satellite imagery tracks currents in Gulf of Mexico. Oil and Gas Journal. 88(19):70-76.

Huh, O.K., W.J. Wiseman, Jr., and L.J. Rouse, Jr. 1978. Winter cycle of sea surface thermal patterns: Northeastern Gulf of Mexico. Journal of Geophysical Research. 83(C9):4523-4529.

Lohrenz, S.E., M.J. Dagg, and T.E. Whitledge. 1990. Enhanced primary production at the plume/oceanic interface of the Mississippi River. Continental Shelf Research. 10(7):639-664.

McClain, E.P., W.G. Pichel, and C.C. Walton. 1985. Comparative performance of AVHRR-based multichannel sea surface temperatures. Journal of Geophysical Research. 90:11,587-11,601.

Milliman, J.D. and R.H. Meade. 1983. World-wide delivery of river sediment to the ocean. Journal of Geology. 91(1):1-21.

Mossa, J. 1990. Discharge-suspended sediment relationship in the Mississippi-Atchafalaya River system, Louisiana. Ph.D. Thesis. Louisiana State University. Baton Rouge, Louisiana. 180 pp.

Muller-Karger F.E., C.R. McClain, and P.L. Richardson. 1988. The dispersal of the Amazon's water. Nature. 333:56-58.

Murray, S.P. 1972. Observations on wind, tidal and density-driven currents in the vicinity of the Mississippi River delta. In Shelf Sediment Transport. Eds. Swift. Duane and Pilkey. Dowden, Hutchinson and Ross, Inc. Stroudsburg, PA. 127-142.

Rabalais, N.N., R.E. Turner, W.J. Wiseman, Jr., and D.F. Boesch. 1991. A brief summary of hypoxia on the northern Gulf of Mexico continental shelf: 1985 - 1988. In R.V. Tyson and T.H. Pearson. Modern and Ancient Continental Shelf Anoxia. pp 35-47.

Rhodes, R.C., A.J. Wallcraft, and J.D. Thompson. 1985. Navy-corrected geostrophic wind set for the Gulf of Mexico. NORDA Technical Note 310. 103 pp.

Roberts, H.H., O.K. Huh, S.A. Hsu, L.J. Rouse, and D. Rickman. 1987. Impact of cold-front passages on geomorphic evolution and sediment dynamics of the complex Louisiana coast. American Society of Civil Engineers. Proceedings of Coastal Sediments '87. pp. 1950-1963.

Rouse, L.J. and J.M. Coleman. 1976. Circulation observations in the Louisiana Bight using LANDSAT imagery. Remote Sensing of Environment. XL:635-642.

Schroeder, W.W., O.K. Huh, L.J. Rouse, Jr., and W.J. Wiseman, Jr. 1985. Satellite observations of the circulation east of the Mississippi Delta: Cold-air outbreak conditions. Remote Sensing of Environment. 18:49-58.

Schroeder, W.W., S.P. Dinnel, W.J. Wiseman, Jr., and W.J. Merrell, Jr. 1987. Circulation patterns inferred from the movement of detached buoys in the eastern Gulf of Mexico. Continental Shelf Research. 7:883-894.

Smith, N.P. 1980. On the hydrography of shelf waters off the central Texas gulf coast. Journal of Physical Oceanography. 10:806-813.

Sogard, S.M., D.E. Hoss, and J.J. Govoni. 1987. Density and depth distribution of larval Gulf menhaden, Brevoortia patronus, Atlantic croaker, Micropogonias undulatus, and spot, Leiostomus xanthurus, in the northern Gulf of Mexico. Fishery Bulletin. 85:601-609.

Stumpf, R.P. 1988. Remote sensing of suspended sediments in estuaries using atmospheric and compositional corrections to AVHRR data. Proceedings of the 21st Intl. Symp. on Remote Sensing of Environment. Ann Arbor. Michigan. 205-222.

Stumpf, R.P. 1992. Remote sensing of water quality in coastal waters. Proceedings of the First Thematic Conference on Remote Sensing for Marine and Coastal Environments. New Orleans, LA. 15-17 June 1992. SPIE 1930:293-305.

Trees, C.C. 1978. Analytical analysis of the effect of dissolved solids on suspended solids determination. Water Pollution Control Federation. Oct. 78:2370-2373.

U.S. Army Corps of Engineers. 1984. Mississippi River, Baton Rouge to the Gulf Louisiana Project. Final Environmental Impact Statement Supplement II. Appendix E. pp. E-9.

U.S. Geological Survey. 1987. Techniques of water-resources investigations of the U.S. Geological Survey. Chapter A4. Methods for collection and analysis of aquatic biological and microbiological samples. Britton, L.J. and P.E. Greeson, Eds. pp 127-130.

Walker, N.D., L.J. Rouse, Jr., O.K. Huh, D.E. Wilensky, and V. Ransibrahmanatal. 1992. Assessing the spatial characteristics and temporal variabilities of the Mississippi and Atchafalaya River plumes. Proceedings of the First Thematic Conference on Remote Sensing for Marine and Coastal Environments. New Orleans, Louisiana. SPIE 1930:719-728.

Walsh, J.J., D.A. Dieterle, M.B. Meyers, and F.E. Muller-Karger. 1989. Nitrogen exchange at the continental margin: A numerical study of the Gulf of Mexico. Progress in Oceanography. 23:245-301.

Wiseman, W.J., Jr. and S.P. Dinnel. 1988. Shelf currents near the mouth of the Mississippi River. Journal of Physical Oceanography. 18:1287-1291.

Wiseman, W.J., Jr., J.M. Bane, S.P. Murray, and M.W. Tubman. 1976. Small-scale temperature and salinity structure over the inner shelf west of the Mississippi River delta. Memoires Societe Royale des Sciences de Liege. 6e serie. tome X. pp277-285.

Wright, L.D. 1970. Ciruculation, effluent diffusion, and sediment transport, mouth of South Pass, Mississippi River delta. Coastal Studies Institute Technical Report. No. 84. Baton Rouge, LA. 60 pp.

Wright, L.D. and J.M. Coleman. 1971. Effluent expansion and interfacial mixing in the presence of a salt wedge, Mississippi River Delta. Journal of Geophysical Research. 76:8649-8661.

Wright, L.D. and J.M. Coleman. 1974. Mississippi River mouth processes: effluent dynamics and morphologic development. Journal of Geology. 82:751-778.

As the Nation's principal conservation agency, the Department of the Interior has responsibility for most of our nationally-owned public lands and natural resources. This includes fostering sound use of our land and water resources; protecting our fish, wildlife, and biological diversity; preserving the environmental and cultural values of our national parks and historical places; and providing for the enjoyment of life through outdoor recreation. The Department assesses our energy and mineral resources and works to ensure that their development is in the best interests of all our people by encouraging stewardship and citizen participation in their care. The Department also has a major responsibility for American Indian reservation communities and for people who live in island territories under U.S. administration.